NSTX

Supported by

U.S. DEPARTMENT OF ENERGY | Office of Science

The Role of Kinetic Effects, Including Plasma Rotation and Energetic Particles, in Resistive Wall Mode Stability

College W&M
Colorado Sch Mines
Columbia U
CompX
General Atomics
INEL
Johns Hopkins U
LANL
LLNL
Lodestar
MIT
Nova Photonics
New York U
Old Dominion U
ORNL
PPPL
PSI
Princeton U
Purdue U
SNL
Think Tank, Inc.
UC Davis
UC Irvine
UCLA
UCSD
U Colorado
U Illinois
U Maryland
U Rochester
U Washington
U Wisconsin

Jack Berkery

Department of Applied Physics, Columbia University, New York, NY, USA

51st Annual Meeting of the Division of Plasma Physics
Atlanta, Georgia
November 3, 2009

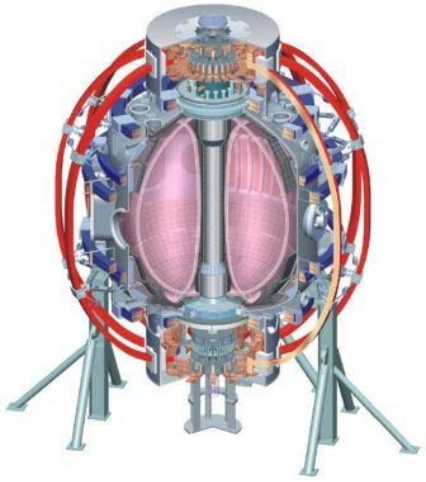

Culham Sci Ctr
U St. Andrews
York U
Chubu U
Fukui U
Hiroshima U
Hyogo U
Kyoto U
Kyushu U
Kyushu Tokai U
NIFS
Niigata U
U Tokyo
JAEA
Hebrew U
Ioffe Inst
RRC Kurchatov Inst
TRINITI
KBSI
KAIST
POSTECH
ASIPP
ENEA, Frascati
CEA, Cadarache
IPP, Jülich
IPP, Garching
ASCR, Czech Rep
U Quebec

NSTX

Supported by

U.S. DEPARTMENT OF ENERGY | Office of Science

In collaboration with:

S.A. Sabbagh, H. Reimerdes

Department of Applied Physics, Columbia University, New York, NY, USA

R. Betti, B. Hu

Laboratory for Laser Energetics, University of Rochester, Rochester, NY, USA

R.E. Bell, S.P. Gerhardt, N. Gorelenkov, B.P. LeBlanc, J. Manickam, M. Podesta

Princeton Plasma Physics Laboratory, Princeton University, Princeton, NJ, USA

K. Tritz

Dept. of Physics and Astronomy, Johns Hopkins University, Baltimore, MD, USA

… and the NSTX team

Supported by:

U.S. Department of Energy Contracts
DE-FG02-99ER54524, DE-AC02-09CH11466, and DE-FG02-93ER54215

College W&M
Colorado Sch Mines
Columbia U
CompX
General Atomics
INEL
Johns Hopkins U
LANL
LLNL
Lodestar
MIT
Nova Photonics
New York U
Old Dominion U
ORNL
PPPL
PSI
Princeton U
Purdue U
SNL
Think Tank, Inc.
UC Davis
UC Irvine
UCLA
UCSD
U Colorado
U Illinois
U Maryland
U Rochester
U Washington
U Wisconsin

Culham Sci Ctr
U St. Andrews
York U
Chubu U
Fukui U
Hiroshima U
Hyogo U
Kyoto U
Kyushu U
Kyushu Tokai U
NIFS
Niigata U
U Tokyo
JAEA
Hebrew U
Ioffe Inst
RRC Kurchatov Inst
TRINITI
KBSI
KAIST
POSTECH
ASIPP
ENEA, Frascati
CEA, Cadarache
IPP, Jülich
IPP, Garching
ASCR, Czech Rep
U Quebec

The resistive wall mode (RWM) is disruptive; it is important to understand the physics of its stabilization

- Motivation
  - The RWM limits plasma pressure and leads to disruptions.
  - Physics of RWM stabilization is key for extrapolation to:
    - sustained operation of a future NBI driven, rotating ST-CTF, and
    - disruption-free operation of a low rotation burning plasma (ITER).
- Outline
  - RWM experimental characteristics in NSTX
  - Kinetic RWM stabilization theory: window of ω_ϕ with weakened stability
  - Comparison of theory and NSTX experimental results
  - The role of energetic particles

The RWM is identified in NSTX by a variety of observations

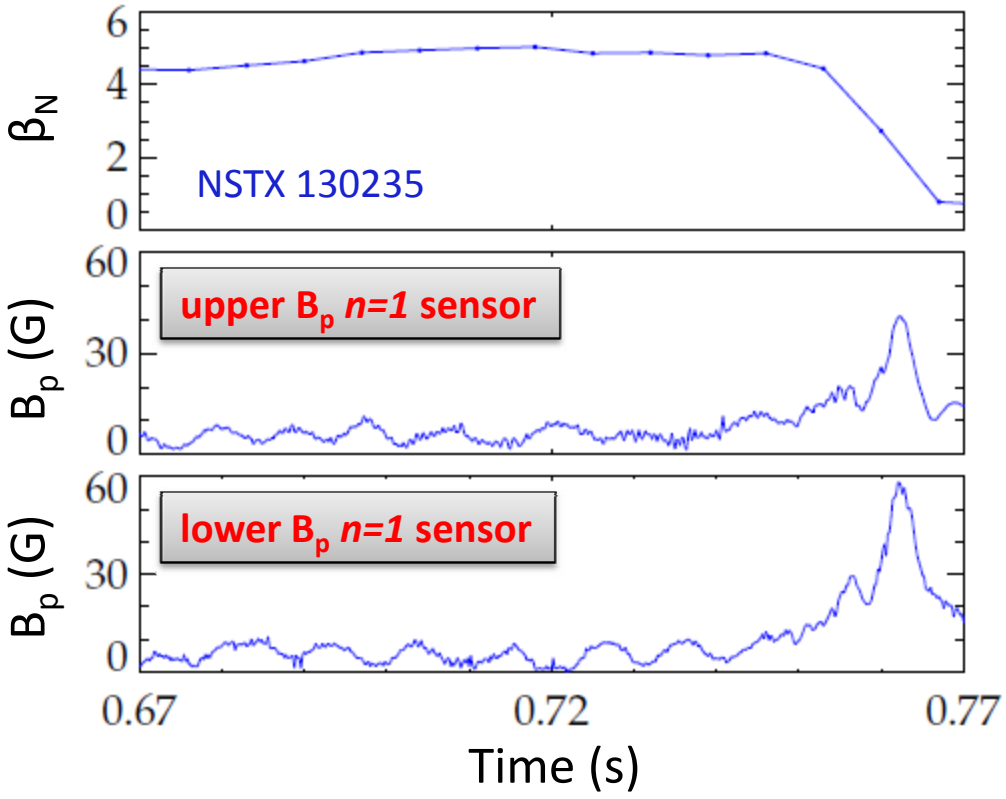

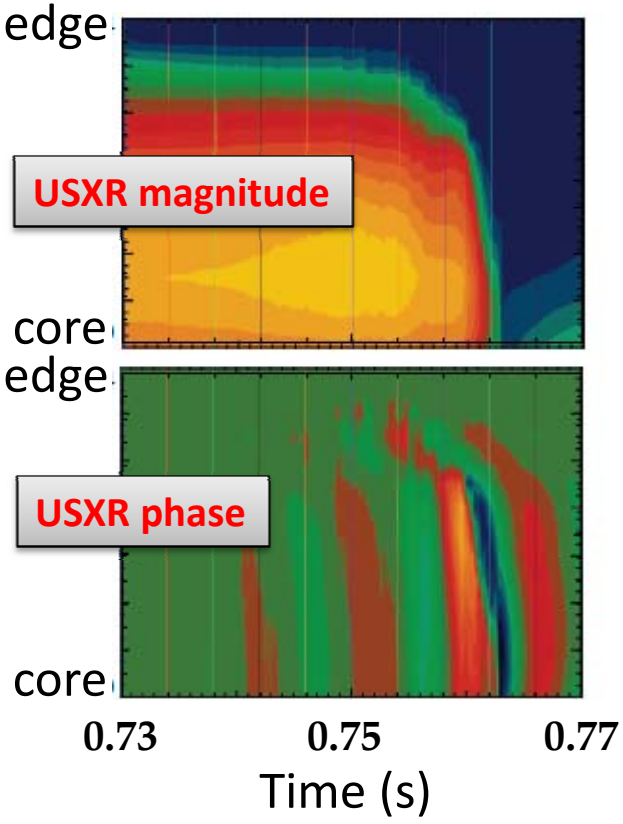

- Growing signal on low frequency poloidal magnetic sensors
- Global collapse in USXR signals, with no clear phase inversion
- Causes a collapse in β and disruption of the plasma

NSTX experimental RWM instability can not be explained by scalar critical rotation theory

In NSTX, the RWM can go unstable with a wide range of toroidal plasma rotation, ω_ϕ.

A.C. Sontag et. al., Nucl. Fus., 47 (2007) 1005

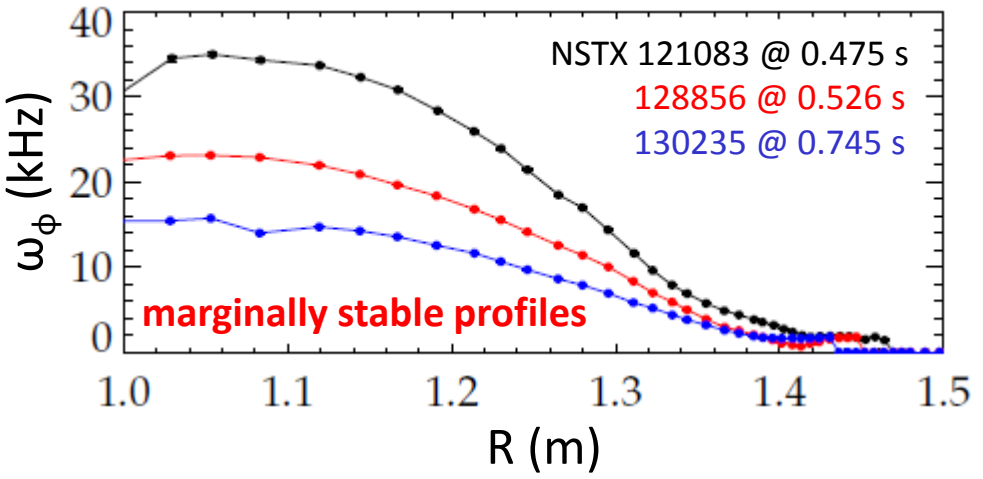

Stable discharges can have very low ω_ϕ.

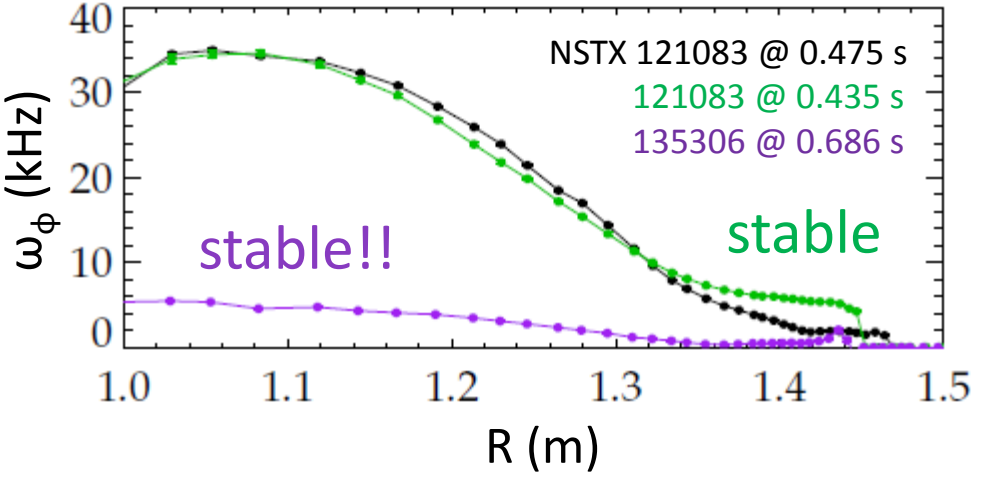

A theoretical model broad enough in scope to explain these results is needed.

Kinetic δW_K term in the RWM dispersion relation provides dissipation that enables stabilization

1. Ideal theory alone shows instability above the no-wall limit:

$$\gamma\tau_w = -\frac{\delta W_\infty}{\delta W_b}$$

2. Dissipation enables stabilization:

$$(\gamma - i\omega_r)\tau_w = -\frac{\delta W_\infty + \delta W_K}{\delta W_b + \delta W_K}$$

(Hu, Betti, and Manickam, PoP, 2005)

3. Calculation of δW_K with the MISK code includes:
   - Trapped Thermal Ions
   - Trapped Electrons
   - Circulating Thermal Ions
   - Alfven Layers (analytic)
   - Trapped Energetic Particles

Typically, trapped thermal ions account for 70-80% of $\mathrm{Re}(\delta W_K)$

The dependence of stability on plasma rotation is complex

Trapped Ions:

$$\delta W_K \sim \left[\frac{(\omega_r + i\gamma)\frac{\partial f}{\partial \varepsilon} + \frac{\partial f}{\partial \Psi}}{\langle \omega_D \rangle + l\omega_b - i\nu_{\text{eff}} + \omega_E - \omega_r - i\gamma} \right]$$

precession drift bounce collisionality E×B

$$\omega_E = \omega_\phi - \omega_{*i}$$

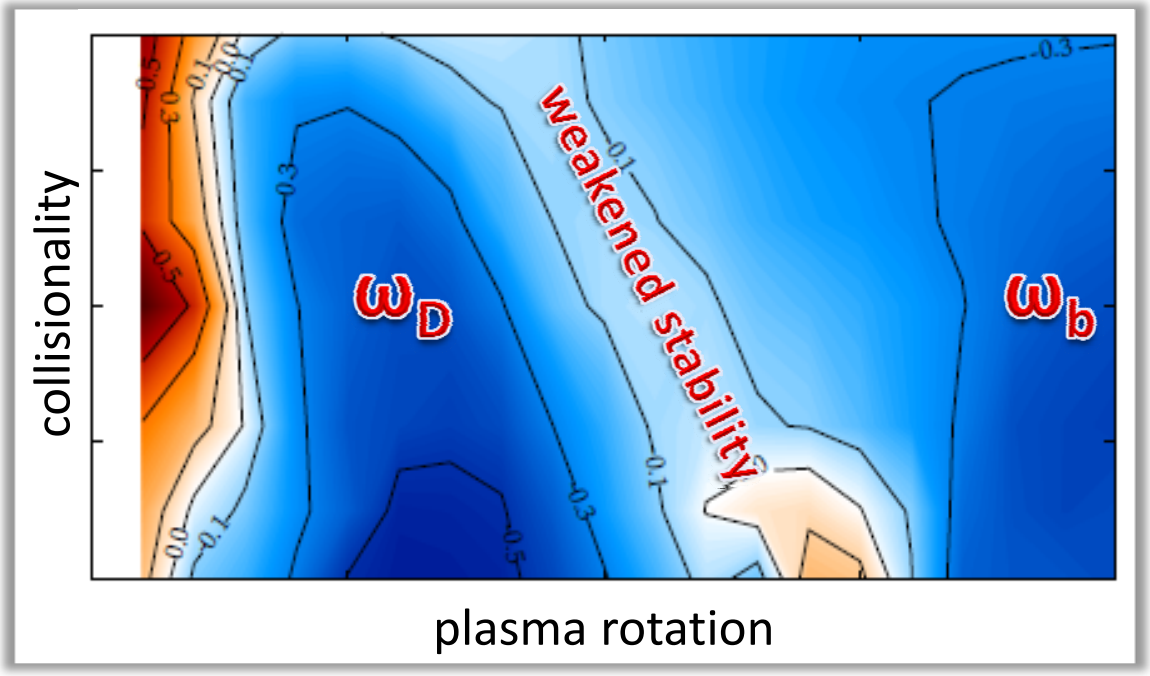

Contours of $\gamma\tau_w$

blue stable

red unstable

white marginal

A window of weakened stability can be found between the bounce and precession drift stabilizing resonances

- What causes this rotation profile to be marginally stable to the RWM?
- Examine relation of ω_ϕ to other frequencies:
  - ℓ=0 harmonic: resonance with precession drift frequency:

$$\omega_E + \langle \omega_D \rangle = 0$$

  - ℓ=-1 harmonic: resonance with bounce frequency:

$$\omega_E + \langle \omega_D \rangle - \omega_b = 0$$

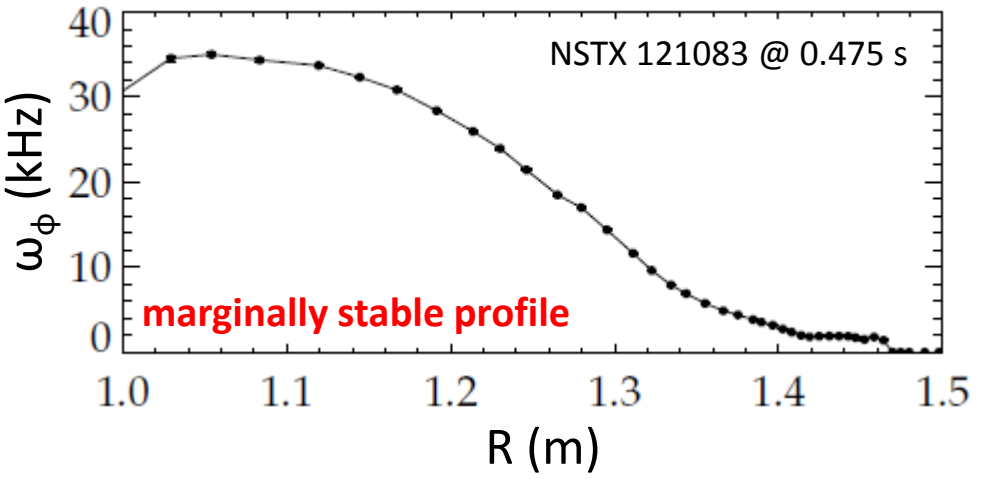

$$\delta W_K \sim \left[\frac{1}{\langle \omega_D \rangle + l\omega_b - i\nu_{\text{eff}} + \omega_E} \right]$$

$$\omega_E = \omega_\phi - \omega_{*i}$$

A window of weakened stability can be found between the bounce and precession drift stabilizing resonances

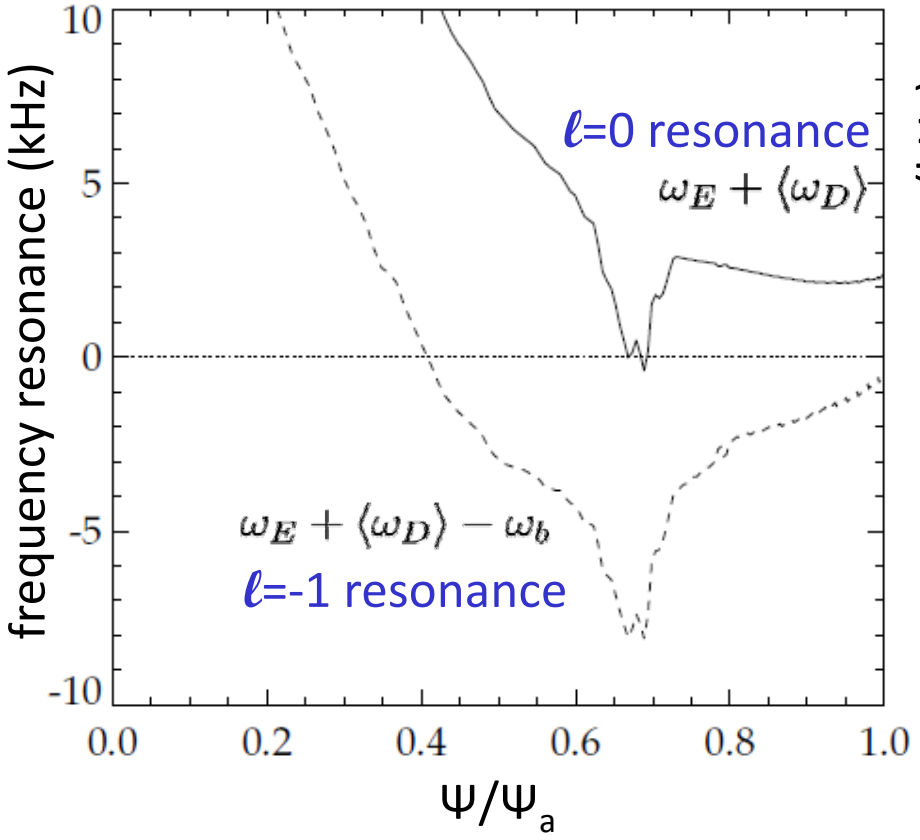

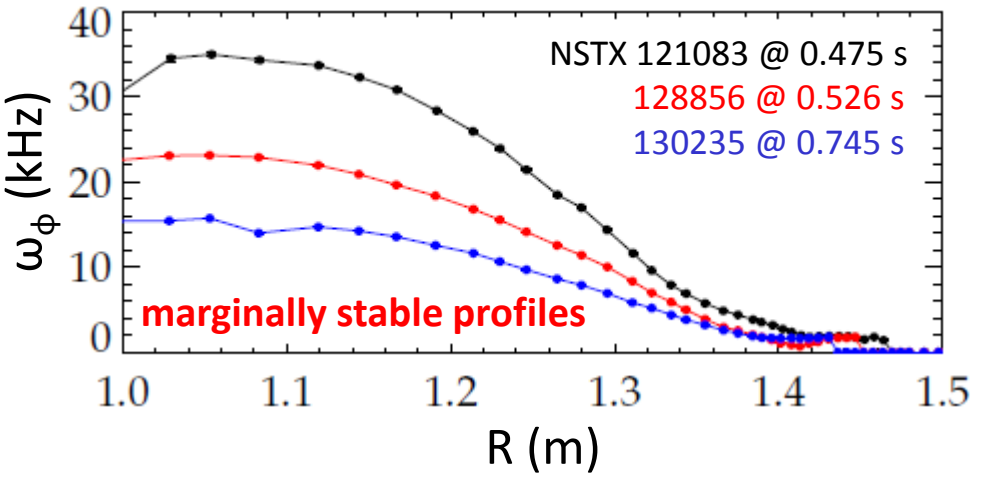

$$\delta W_K \sim \left[\frac{1}{\langle\omega_D\rangle + l\omega_b - i\nu_{\text{eff}} + \omega_E}\right]$$

$$\omega_E = \omega_\phi - \omega_{*i}$$

- The experimentally marginally stable ω_ϕ profile is in-between the stabilizing resonances.
  - Is this true for each of the widely different unstable profiles?

A window of weakened stability can be found between the bounce and precession drift stabilizing resonances

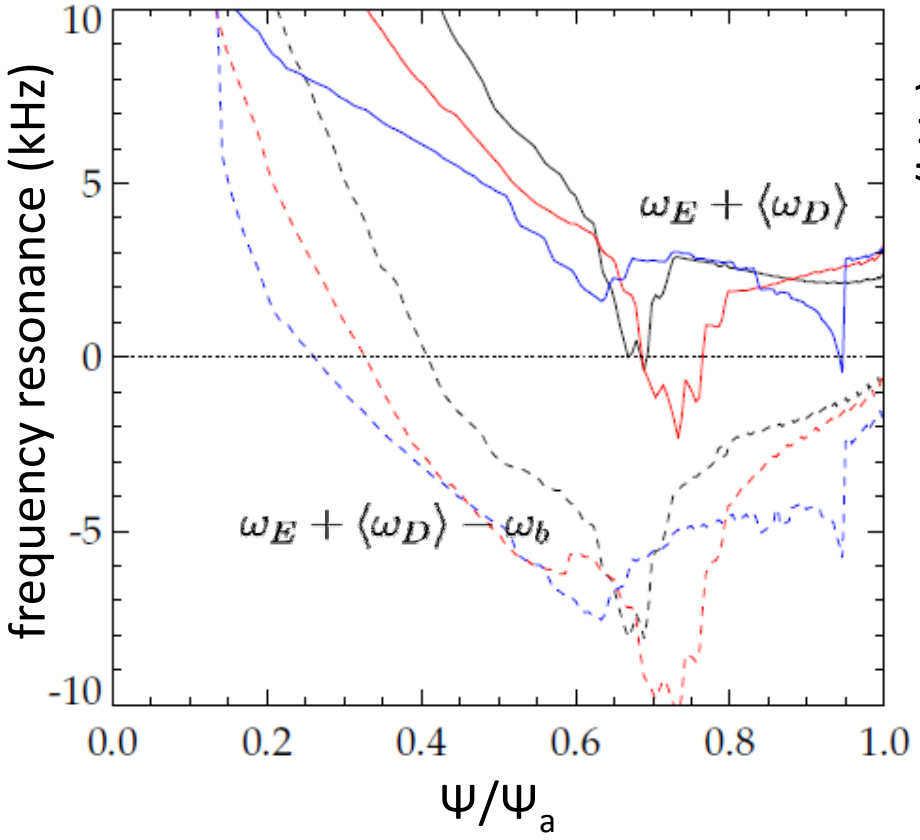

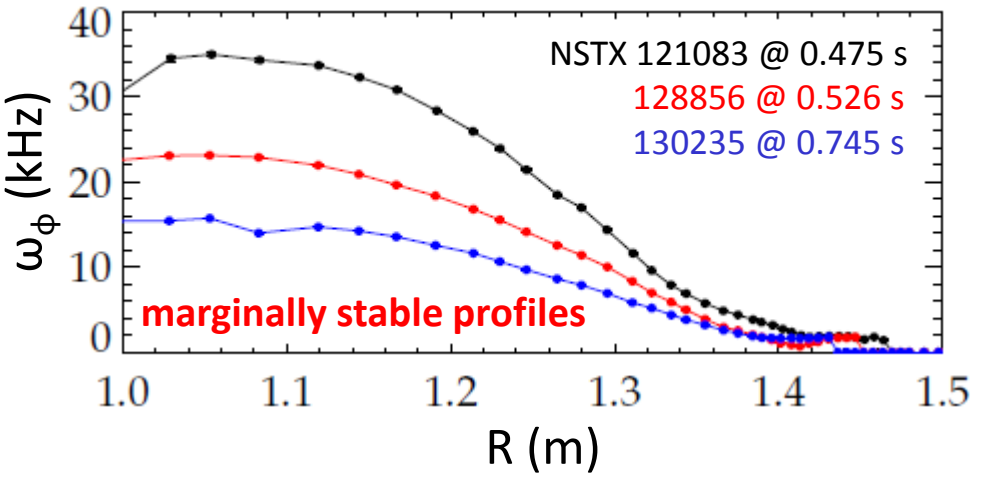

$$\delta W_K \sim \left[\frac{1}{\langle\omega_D\rangle + l\omega_b - i\nu_{\text{eff}} + \omega_E}\right]$$

$$\omega_E = \omega_\phi - \omega_{*i}$$

- The experimentally marginally stable ω_ϕ profile is in-between the stabilizing resonances.
  - Is this true for each of the widely different unstable profiles: Yes

When the rotation is in resonance, the plasma is stable

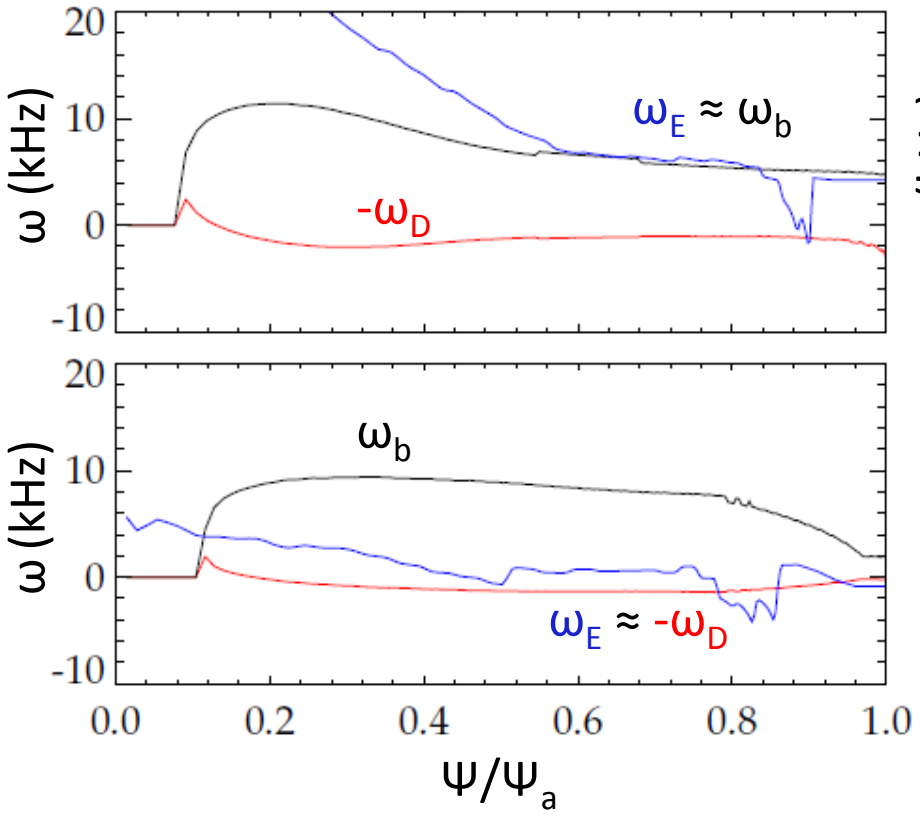

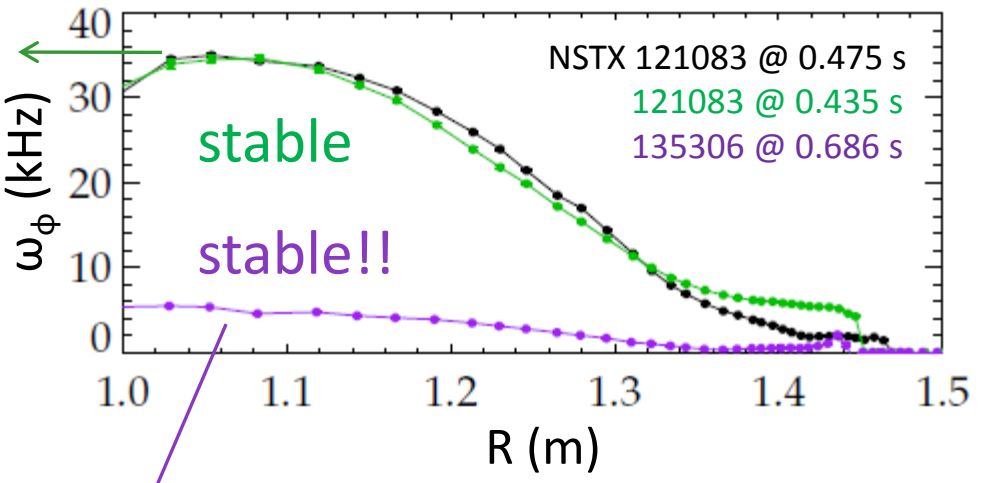

$$\delta W_K \sim \left[\frac{1}{\langle\omega_D\rangle + l\omega_b - i\nu_{\text{eff}} + \omega_E}\right]$$

$$\omega_E = \omega_\phi - \omega_{*i}$$

- Stable cases in bounce resonance at high rotation
- Stable cases in precession drift resonance at low rotation

Full MISK calculation shows that trapped thermal ions are the most important contributors to stability

$$\delta W_K = \frac{\sqrt{\pi}}{2} \sum_{\pm\sigma} \int_0^{\Psi_a} \frac{d\Psi}{B_0}(nT) \sum_{l=-\infty}^{\infty} \int_{B_0/B_{max}}^{B_0/B_{min}} d\Lambda \hat{\tau}$$
$$\times \int_0^{\infty} \left[\frac{\omega_{*N} + \left(\hat{\varepsilon} - \frac{3}{2}\right)\omega_{*T} + \omega_E - \omega - i\gamma}{\langle \omega_D \rangle + l\omega_b - i\nu_{\text{eff}} + \omega_E - \omega - i\gamma} \right] \hat{\varepsilon}^{5/2} e^{-\hat{\varepsilon}} d\hat{\varepsilon}$$
$$\times \left| \left\langle \left(2 - 3\frac{\Lambda}{B_0/B}\right)(\kappa \cdot \xi_\perp) - \left(\frac{\Lambda}{B_0/B}\right)(\nabla \cdot \xi_\perp) \right\rangle \right|^2$$

Full δW_K eqn. for trapped thermal ions

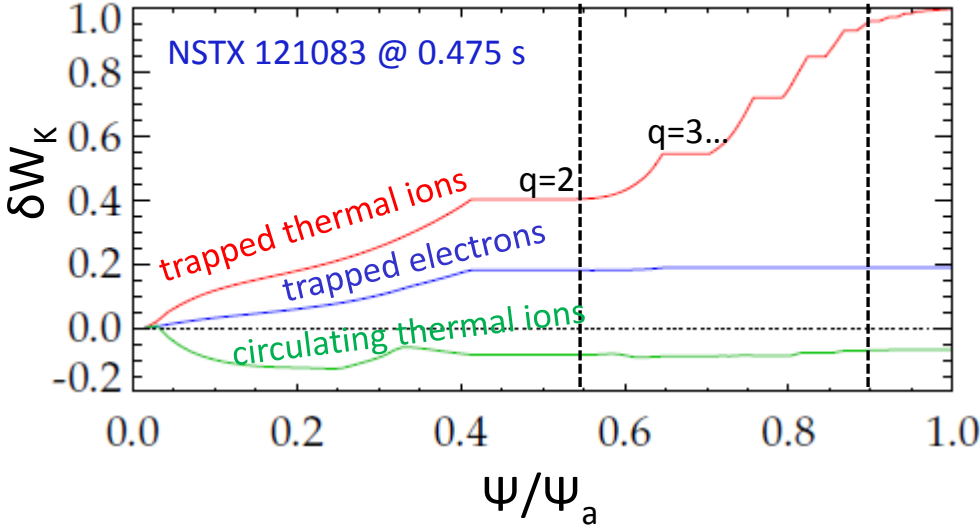

- Examine δW_K from each particle type vs. Ψ
  - Thermal ions are the most important contributor to stability.
  - Flat areas are rational surface layers (integer q ± 0.2).
- Entire profile is important, but q > 2 contributes ~60%
  - RWM eigenfunction and temperature, density gradients are large in this region.

The dispersion relation can be rewritten in a form convenient for making stability diagrams

Contours of γ form circles on a stability diagram of $\mathrm{Im}(\delta W_K)$ vs. $\mathrm{Re}(\delta W_K)$.

$$(\gamma - i\omega_r)\tau_w = -\frac{\delta W_\infty + \delta W_K}{\delta W_b + \delta W_K} \quad \Rightarrow \quad (Re\,(\delta W_K) - a)^2 + (Im\,(\delta W_K))^2 = r^2$$

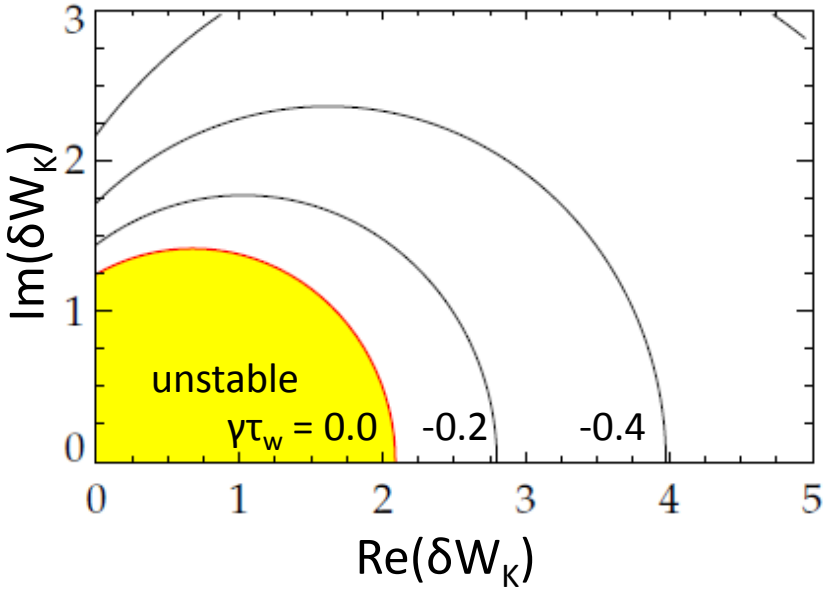

Let us now scale the experimental rotation profile to illuminate the complex relationship between rotation and stability

Scaling the experimental rotation profile illuminates the complex relationship between rotation and stability

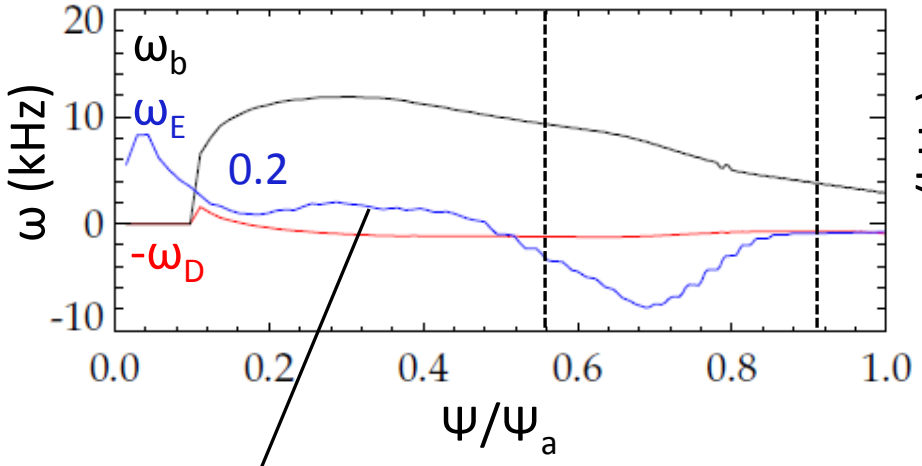

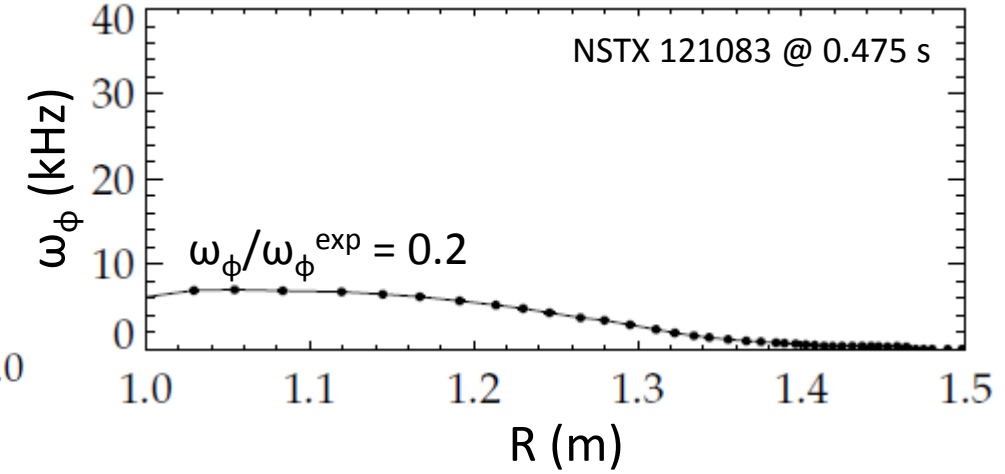

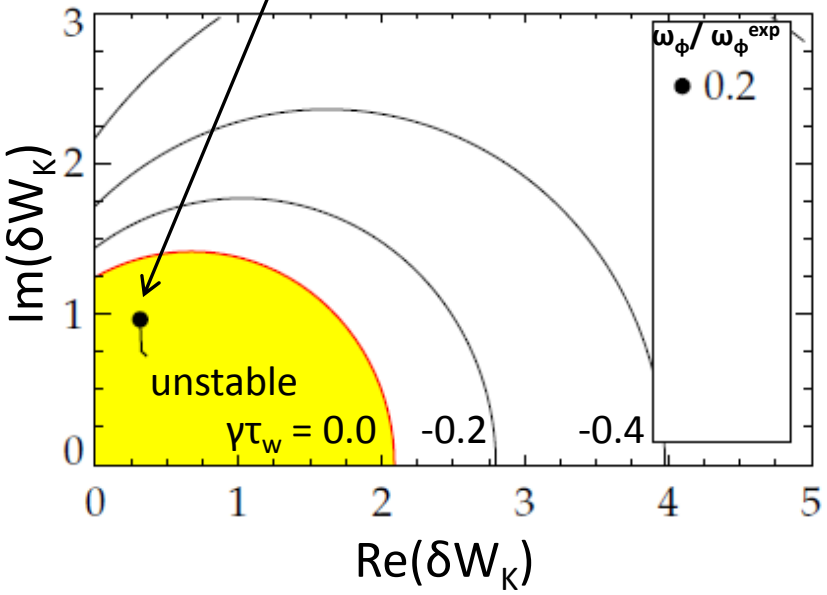

- Rotation profile scan:
  - 0.2: Instability at low rotation.

Scaling the experimental rotation profile illuminates the complex relationship between rotation and stability

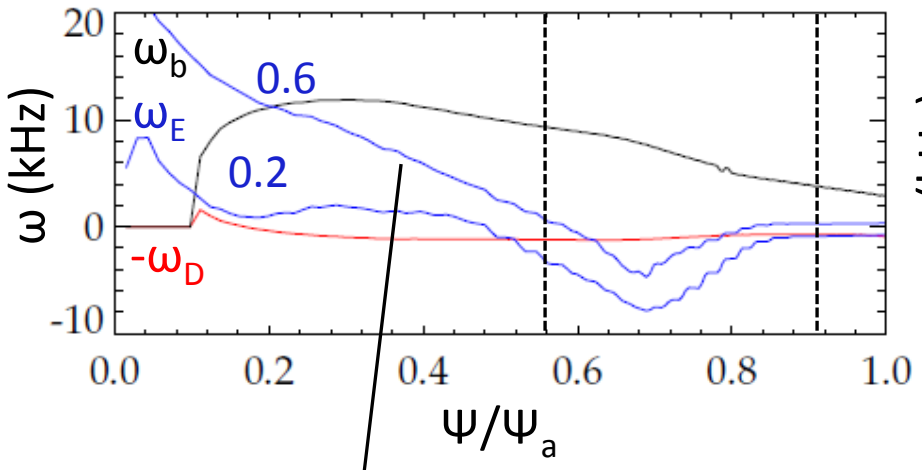

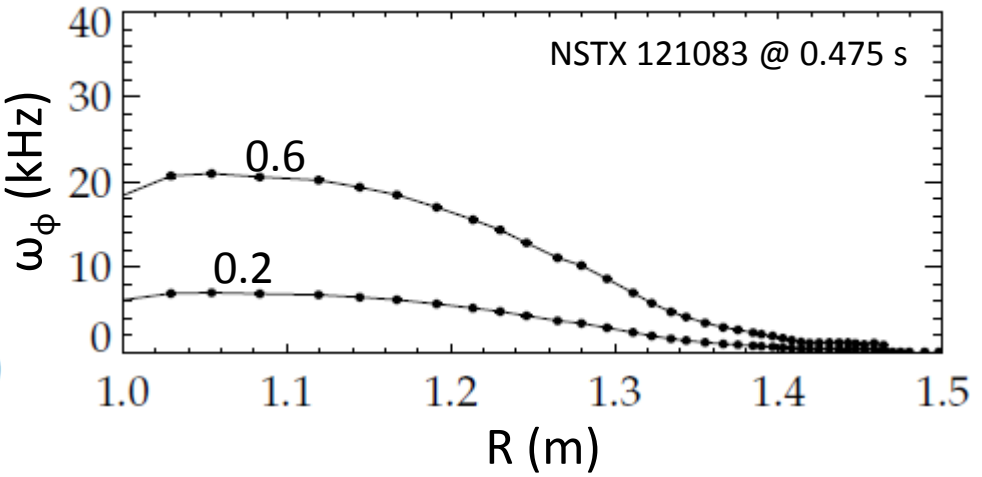

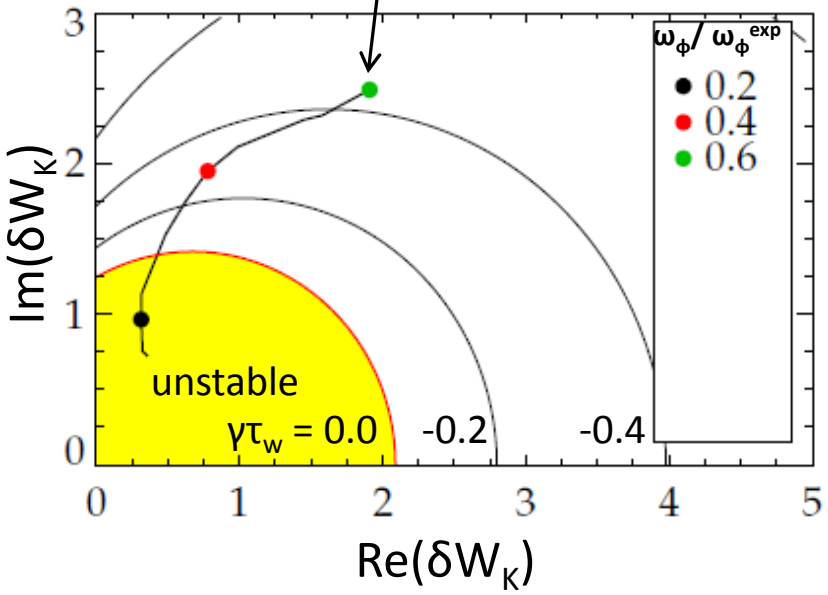

- Rotation profile scan:
  - 0.2: Instability at low rotation.
  - 0.6: Stable: ω_D resonance.

Scaling the experimental rotation profile illuminates the complex relationship between rotation and stability

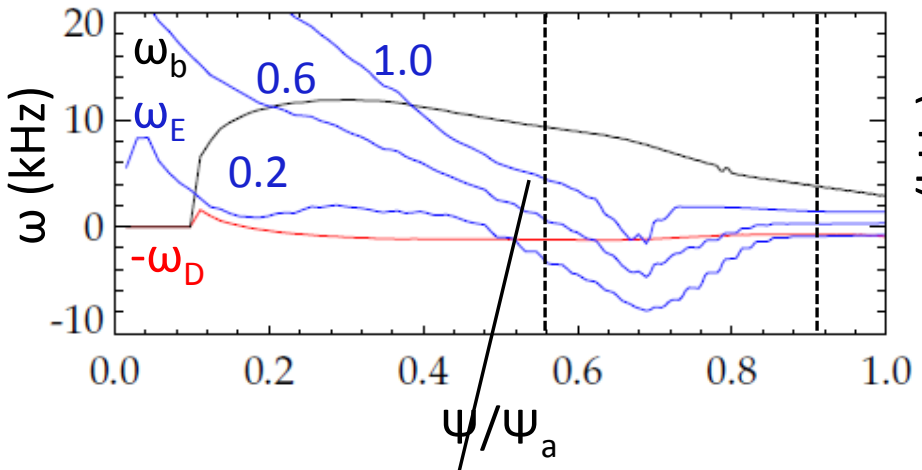

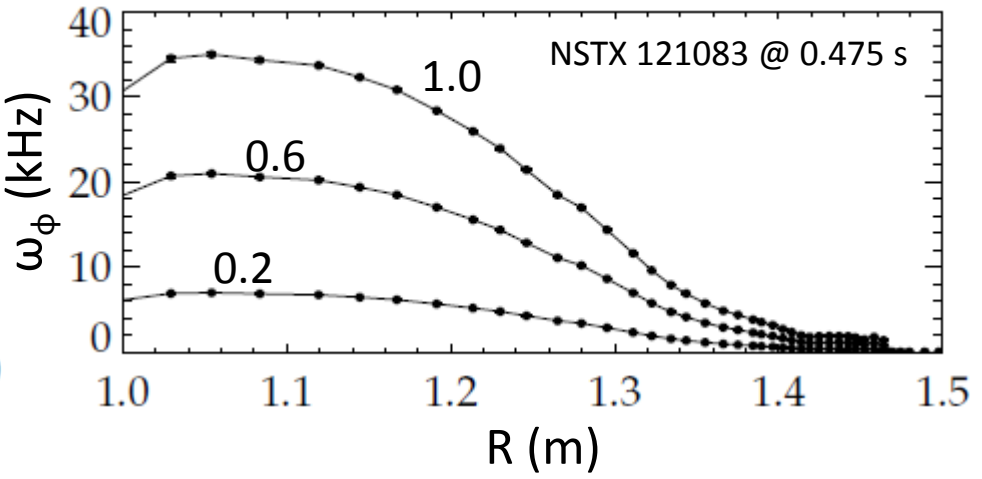

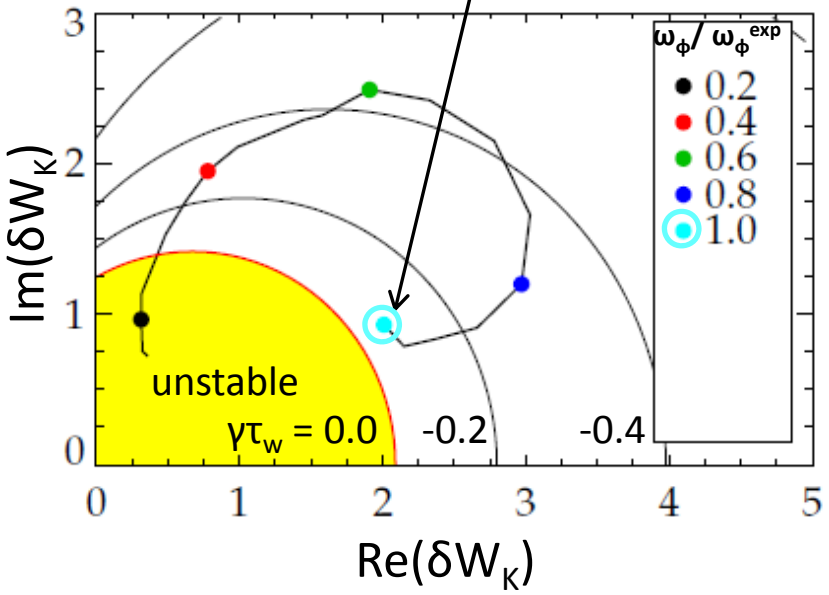

- Rotation profile scan:
  - 0.2: Instability at low rotation.
  - 0.6: Stable: ω_D resonance.
  - 1.0: Marginal: in-between resonances (actual experimental instability).

Scaling the experimental rotation profile illuminates the complex relationship between rotation and stability

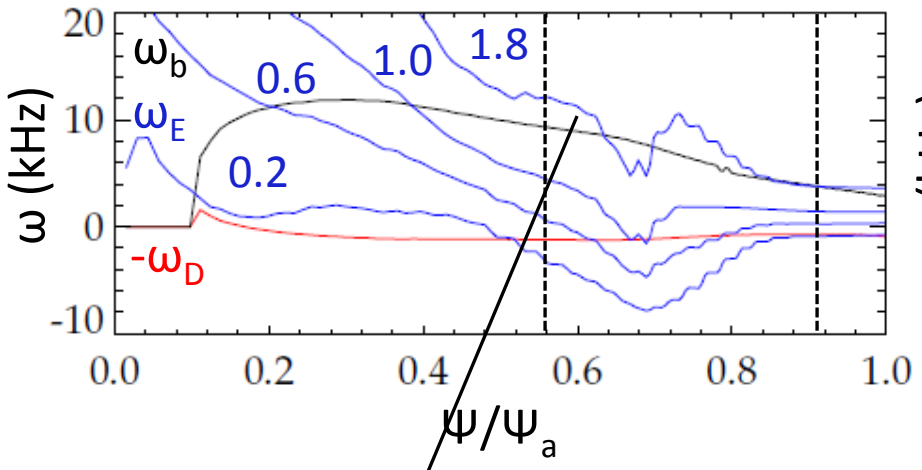

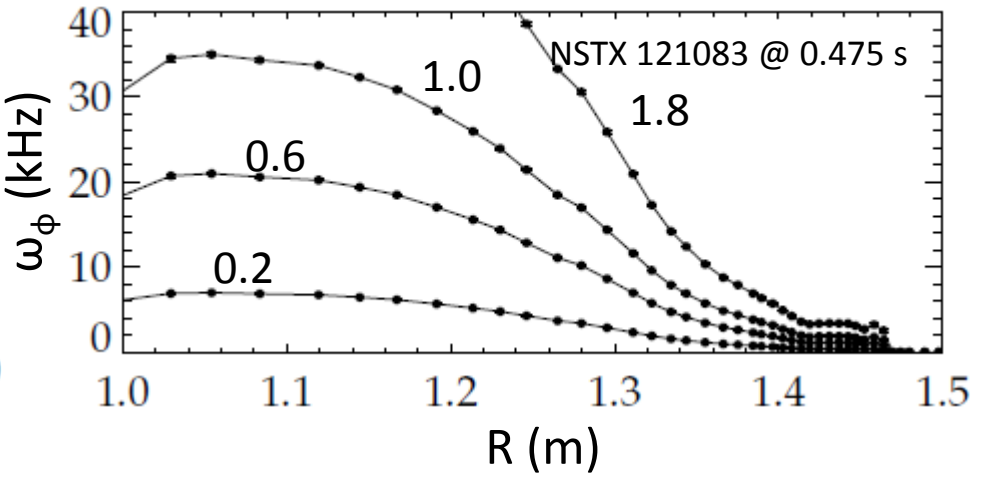

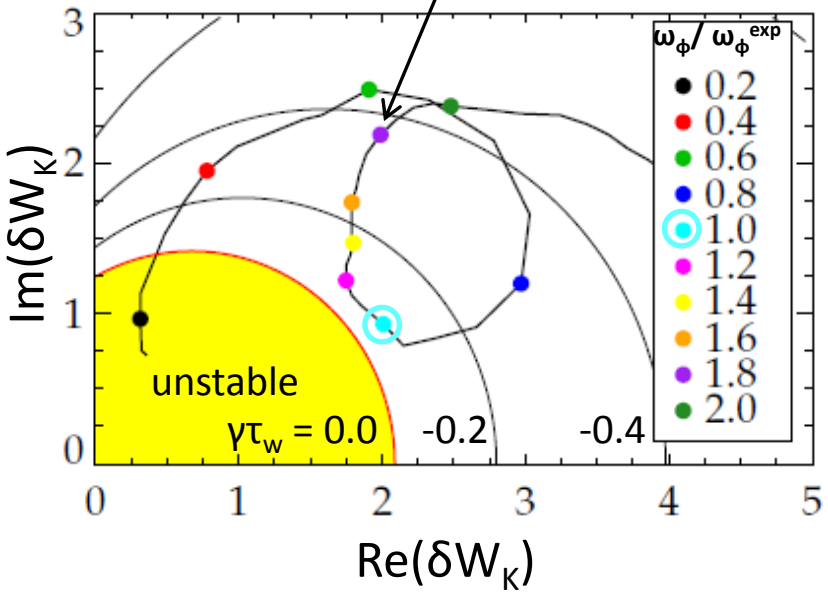

- Rotation profile scan:
  - 0.2: Instability at low rotation.
  - 0.6: Stable: ω_D resonance.
  - 1.0: Marginal: in-between resonances (actual experimental instability).
  - 1.8: Stable: ω_b resonance.

The weakened stability rotation gap is altered by changing collisionality

- Scan of ω_ϕ and collisionality
  - scale *n* & *T* at constant β
  - Changing *v* shifts the rotation of weakened stability.

$$\delta W_K \sim \left[\frac{1}{\langle\omega_D\rangle + l\omega_b - i\nu_{\text{eff}} + \omega_E}\right]$$

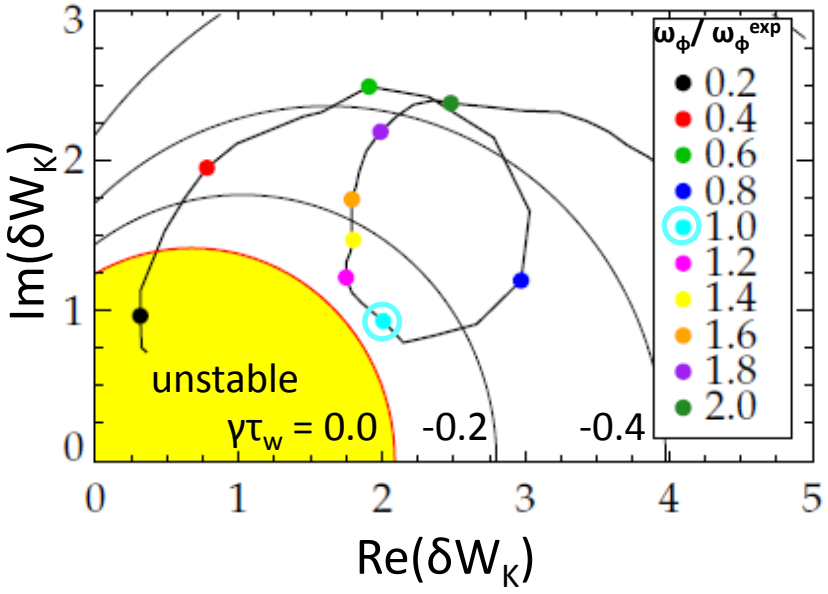

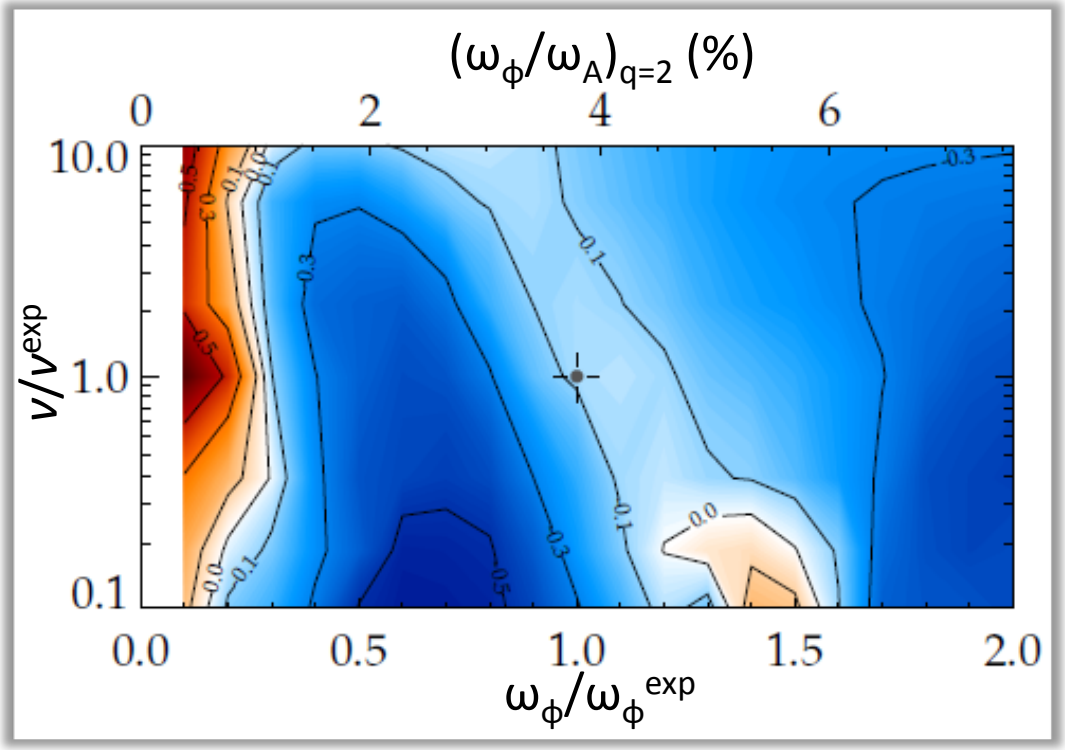

The weakened stability rotation gap is altered by changing collisionality

- Scan of ω_ϕ and collisionality
  - scale *n* & *T* at constant β
  - Changing *v* shifts the rotation of weakened stability.

$$\delta W_K \sim \left[\frac{1}{\langle\omega_D\rangle + l\omega_b - i\nu_{\text{eff}} + \omega_E}\right]$$

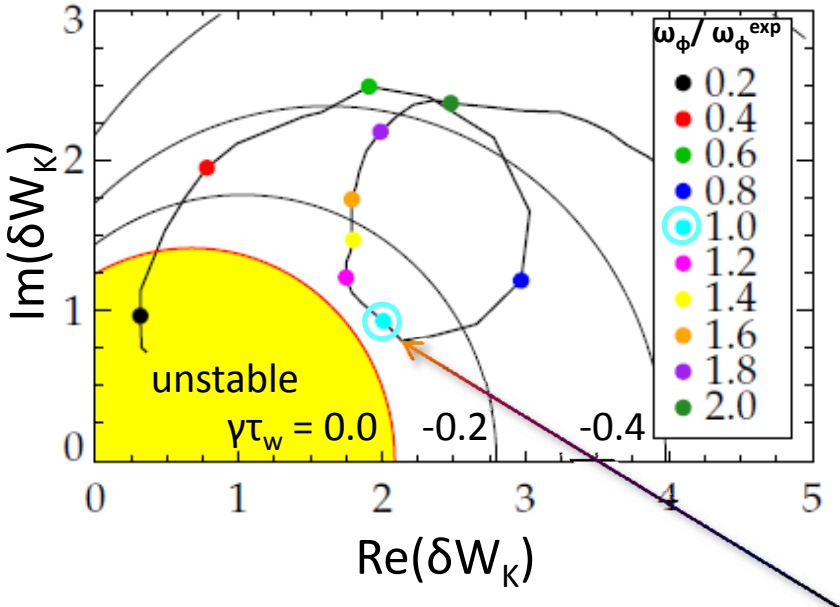

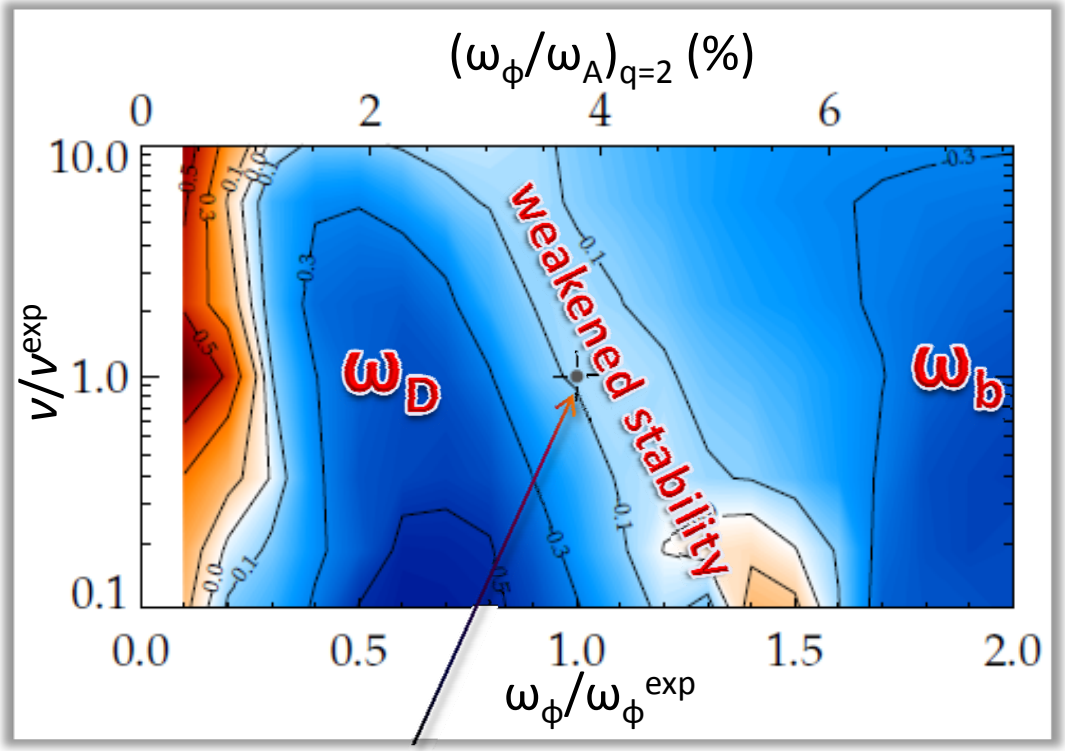

NSTX exp. instability

Widely different experimentally marginally stable rotation profiles each are in the gap between stabilizing resonances

- Sometimes the stability reduction is not enough to quantitatively reach marginal
- Investigating sensitivities to inputs.

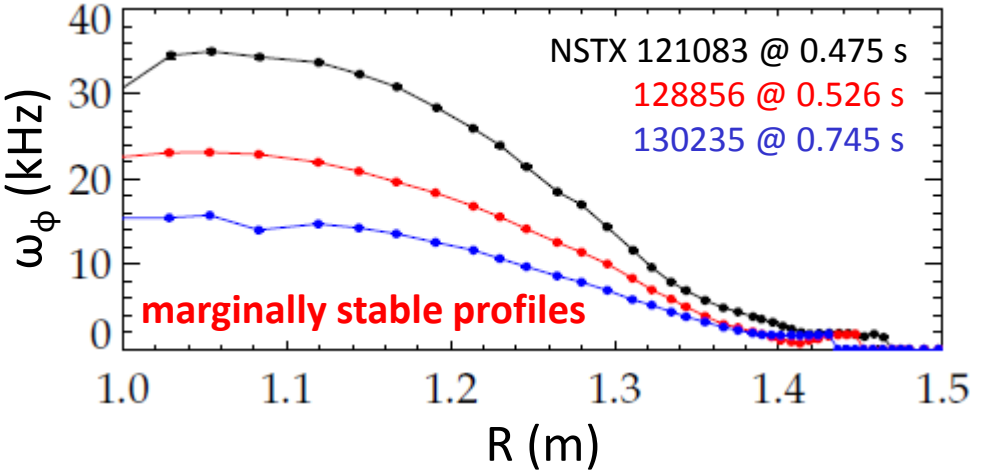

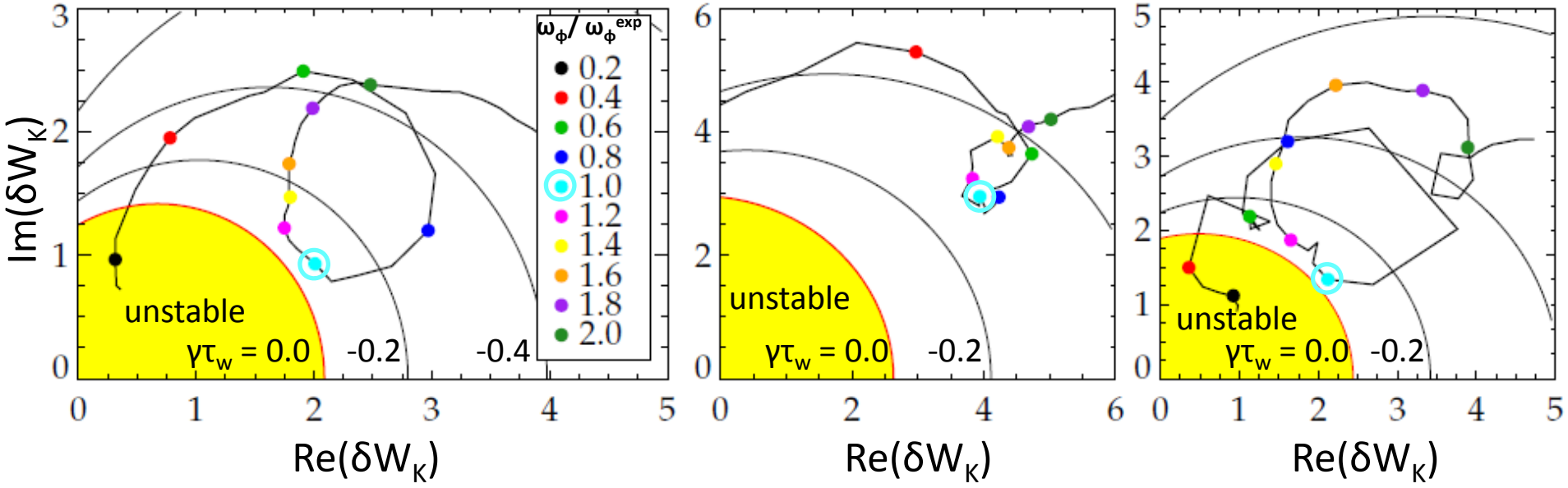

121083 @ 0.475 s | 128856 @ 0.526 s | 130235 @ 0.745 s

Widely different experimentally marginally stable rotation profiles each are in the gap between stabilizing resonances

- Sometimes the stability reduction is not enough to quantitatively reach marginal
- Investigating sensitivities to inputs. ex: Δq = 0.15 – 0.25

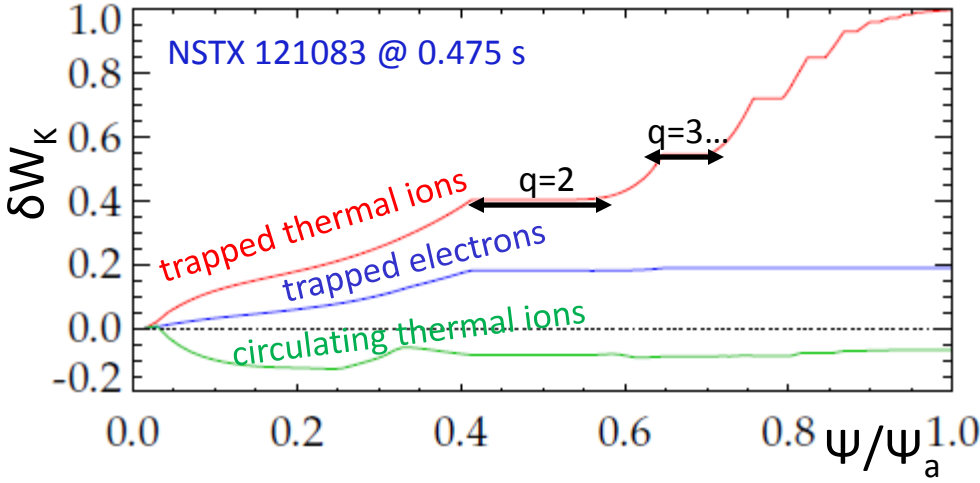

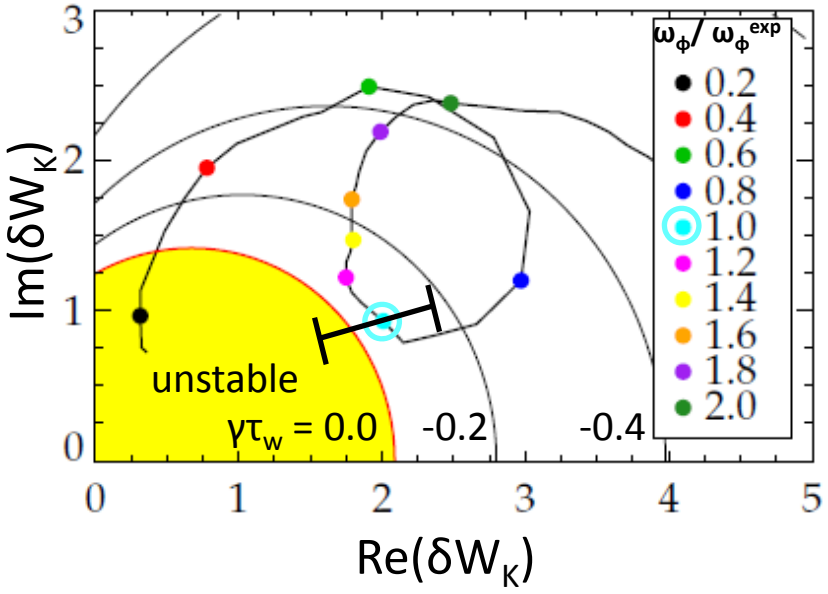

121083 @ 0.475 s

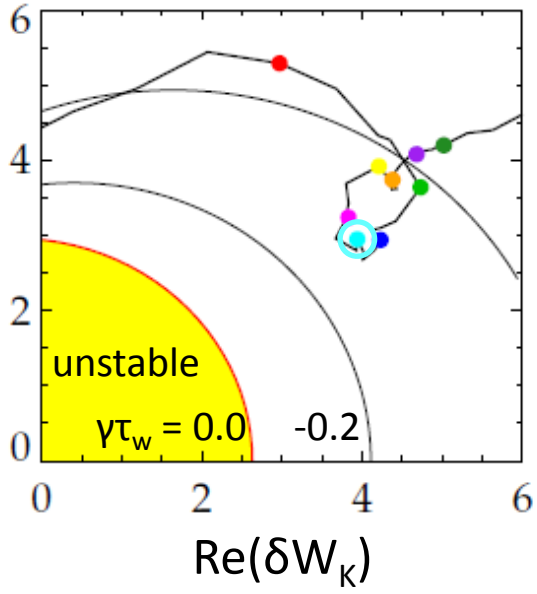

128856 @ 0.526 s

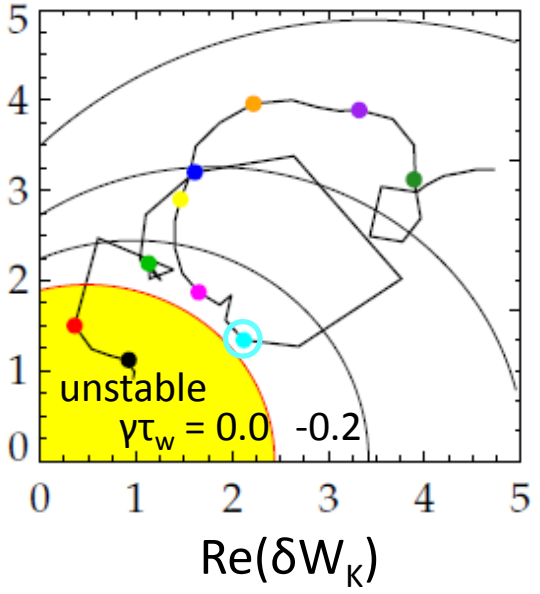

130235 @ 0.745 s

Present inclusion of energetic particles in MISK: isotropic slowing down distribution (ex. alphas in ITER)

Thermal Particles: Maxwellian

$$\delta W_K \sim \left[\frac{(\omega_r + i\gamma)\frac{\partial f}{\partial \varepsilon} + \frac{\partial f}{\partial \Psi}}{\langle \omega_D \rangle + l\omega_b - i\nu_{\text{eff}} + \omega_E - \omega_r - i\gamma} \right]$$

E.P.s: Slowing-down

$$f(\varepsilon, \Psi) = \frac{C(\Psi)}{\varepsilon^{\frac{3}{2}} + \varepsilon_c^{\frac{3}{2}}}$$

- Energetic particles add to δW_K, lead to greater stability
- Example: α particles in ITER
  - Higher β_α leads to greater stability
  - Isotropic f is a good approx.

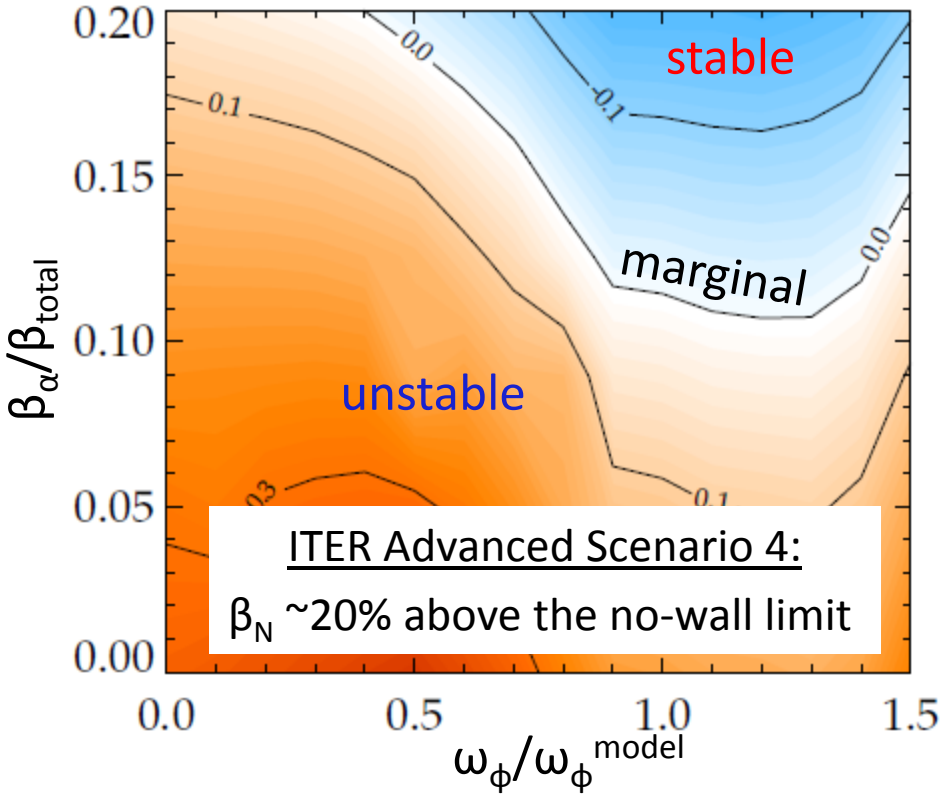

Energetic particles provide a stabilizing force that is independent of rotation and collisionality

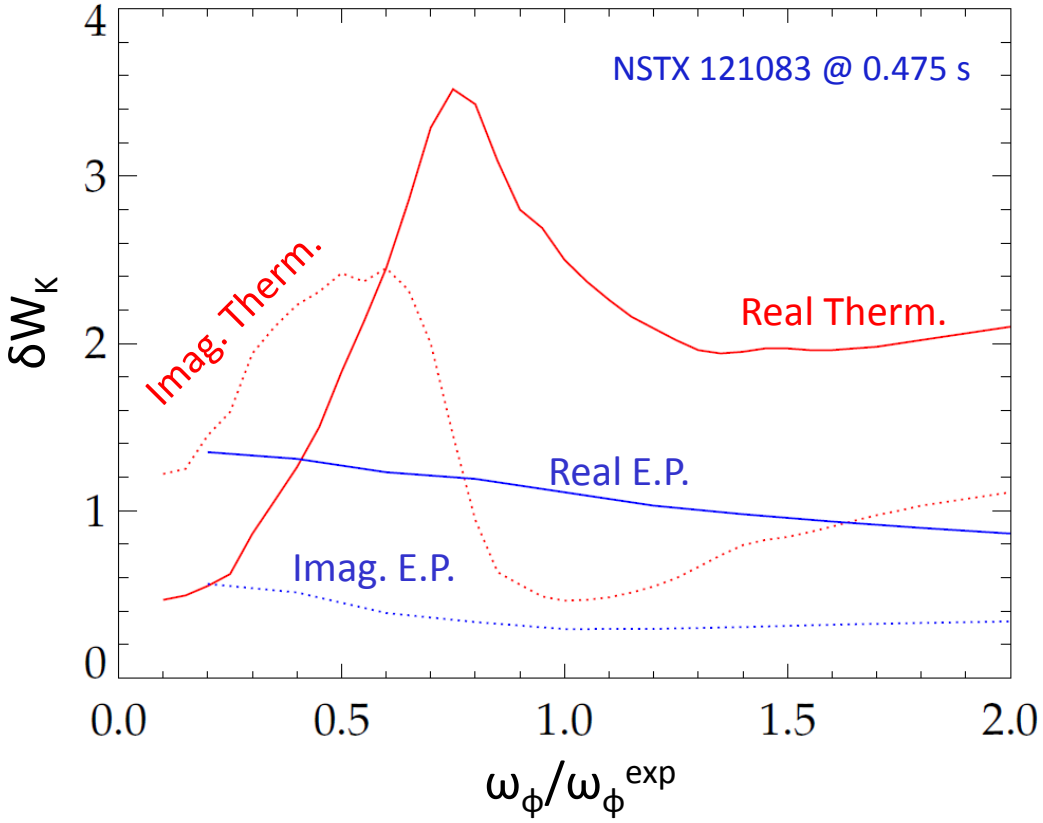

for energetic particles:

$$\delta W_K \sim \left[\frac{1}{\langle\omega_D\rangle + l\omega_b - i\nu_{\text{eff}} + \omega_E}\right]$$

small

- Significant Re(δW_K), but nearly independent of ω_ϕ
- Energetic particles are not in mode resonance
- Effect is not energy dissipation, but rather a restoring force

NSTX experiment in 2009 found that energetic particles contribute linearly to RWM stability

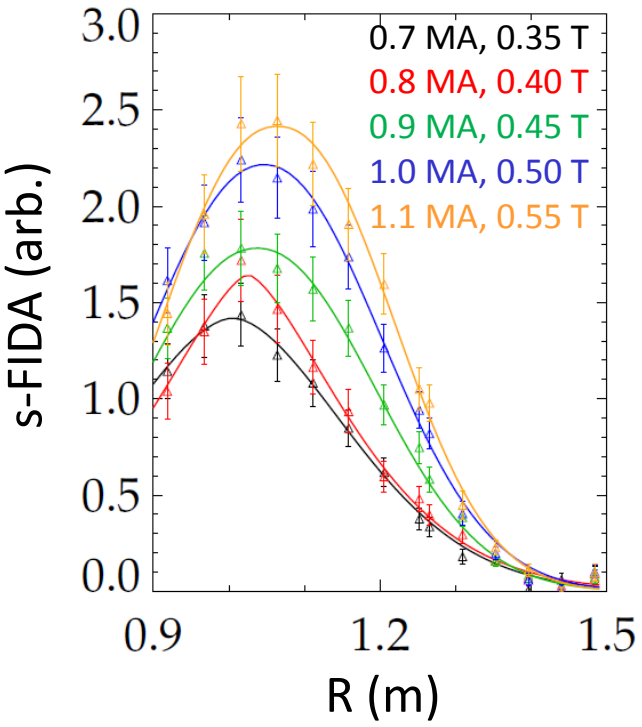

Change in growth rate from energetic particles

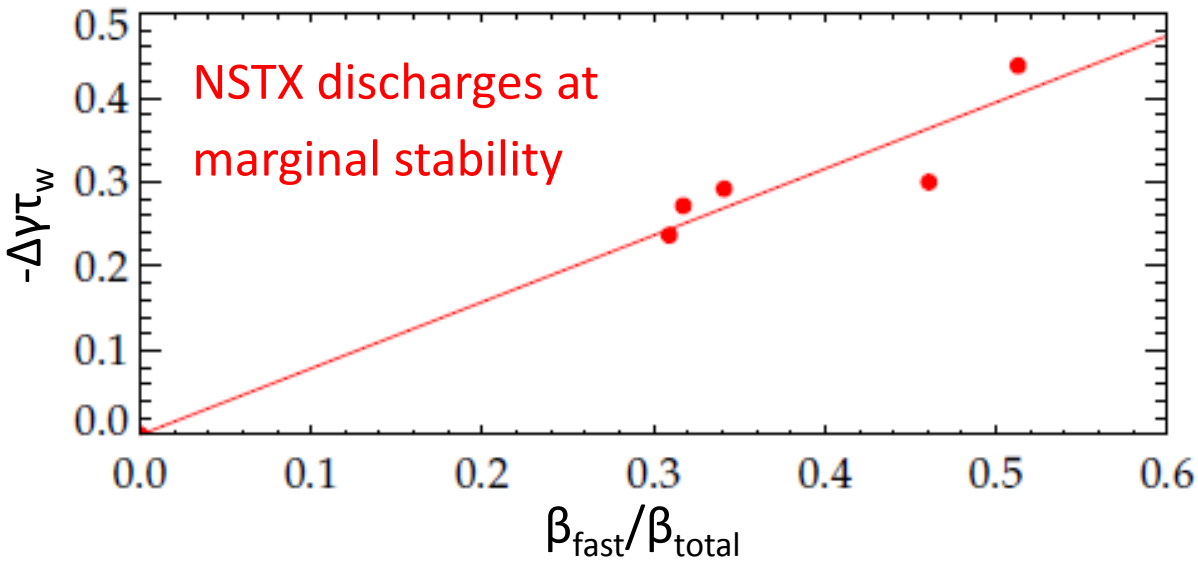

- Despite the additional theoretical stability, these shots experimentally went unstable
  - Investigating whether stabilization from thermal particles is overpredicted by MISK.
  - The overprediction of -Δγ from E.P.s is under investigation…

A new, more accurate energetic particle distribution function is being implemented

- Presently f is considered independent of pitch angle
  - Not a good approximation for beam ions
  - Overpredicts stabilizing trapped fraction
- Towards better quantitative agreement:
  - Use f from TRANSP directly

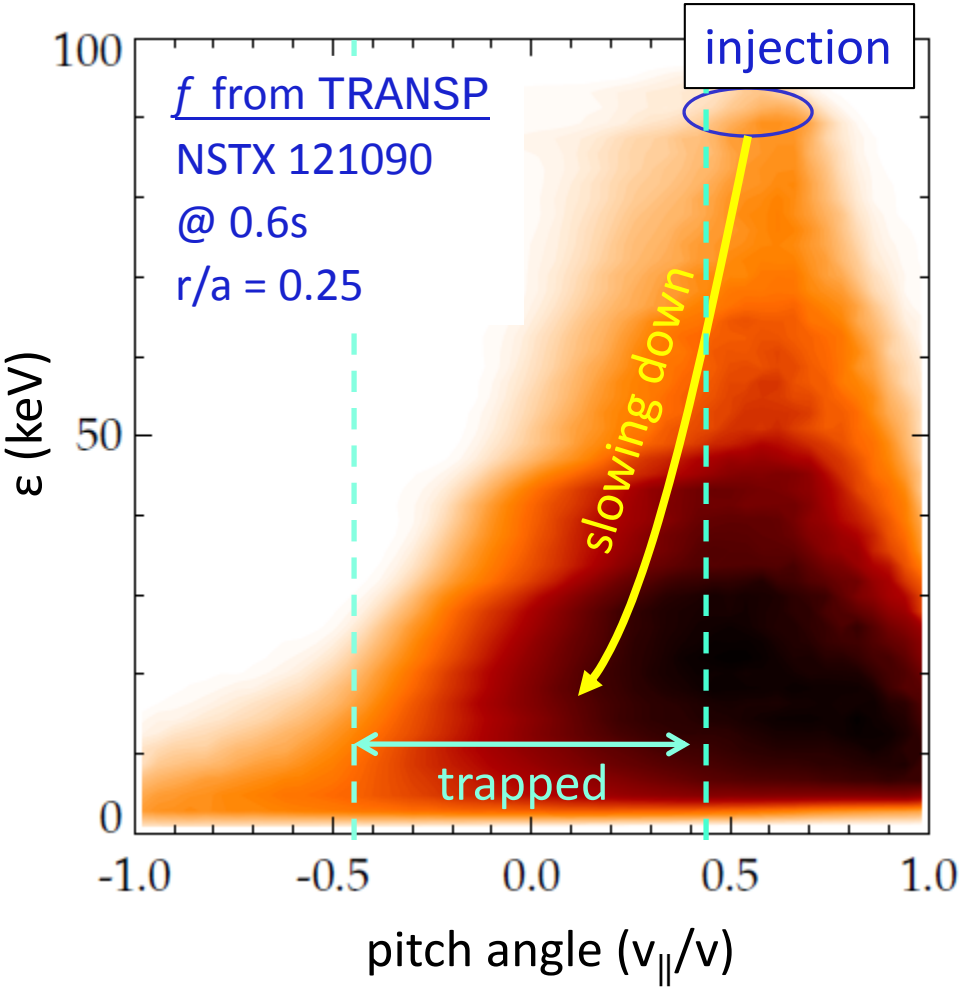

Kinetic RWM stability theory can explain complex relationship of marginal stability with ω_ϕ

- High plasma rotation alone is inadequate to ensure RWM stability in future devices
  - A weakened stability gap in ω_ϕ exists between ω_b and ω_D resonances.
  - Use ω_ϕ control to stay away from, and active control to navigate through gap.
- Favorable comparison between NSTX experimental results and theory
  - Multiple NSTX discharges with widely different marginally stable ω_ϕ profiles fall in this gap.
- Energetic particles provide an important stabilizing effect
  - Works towards quantitative agreement with experiment is ongoing.

Visit the poster this afternoon for more detail

Zooming in on rotation near the edge

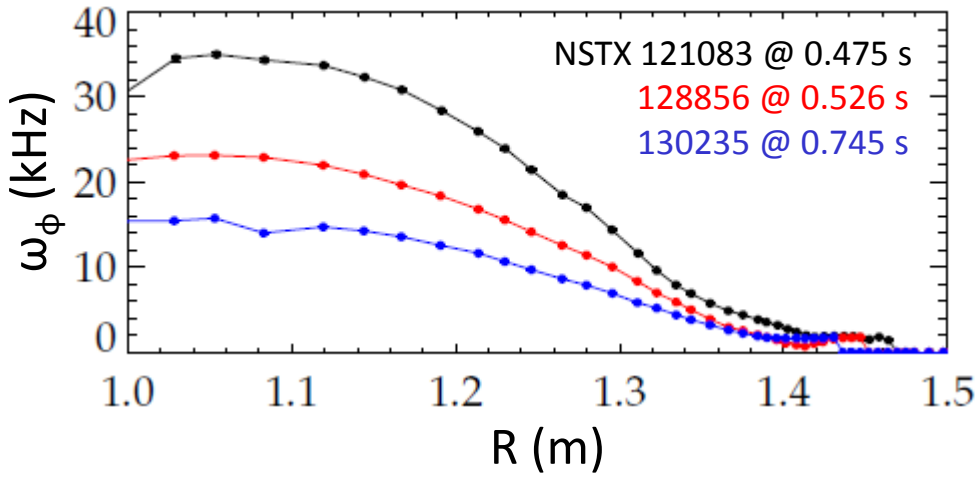

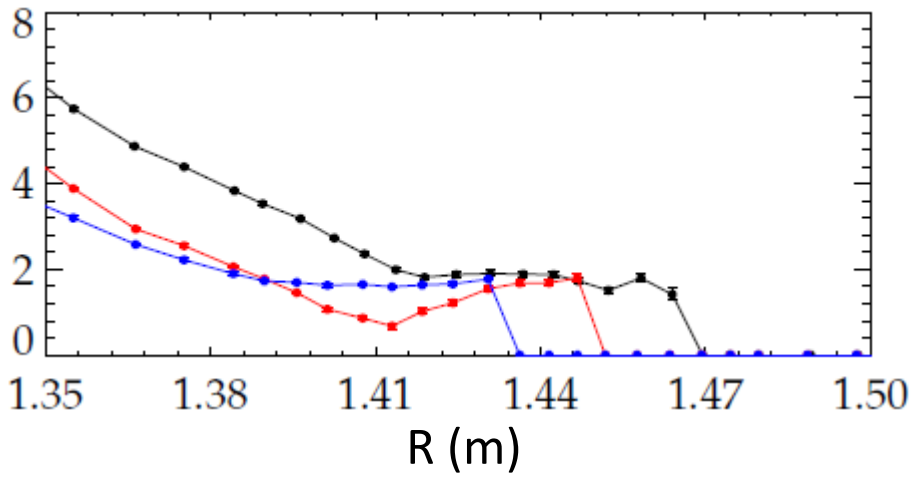

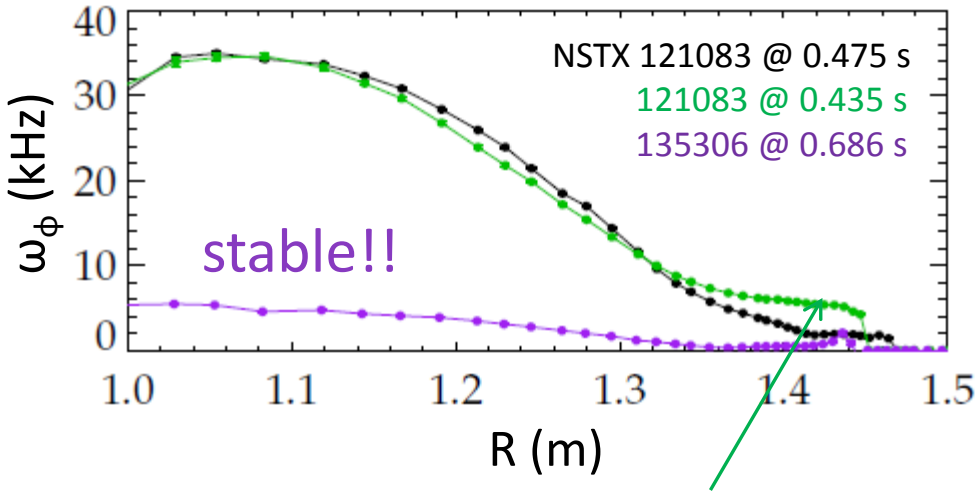

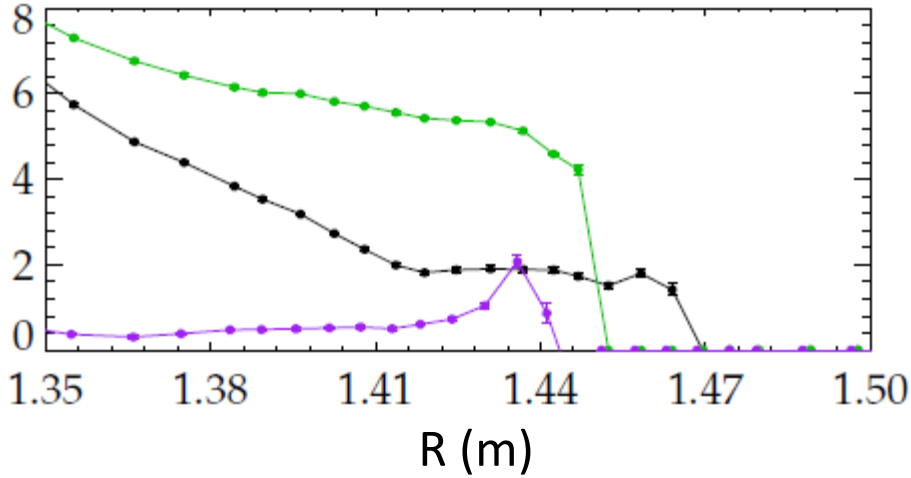

stable 40ms earlier

Kinetic RWM stability theory may explain complex relationship of marginal stability with ω_ϕ

- High plasma rotation alone is inadequate to ensure RWM stability in future devices
  - A weakened stability gap exists between ω_b and ω_D resonances.
  - Use ω_ϕ control to stay away from, and active control to navigate through gap.
- Favorable comparison between NSTX exp. results and theory
  - Multiple NSTX discharges with different marginally stable ω_ϕ profiles fall in this gap
- Energetic particles provide an important stabilizing effect

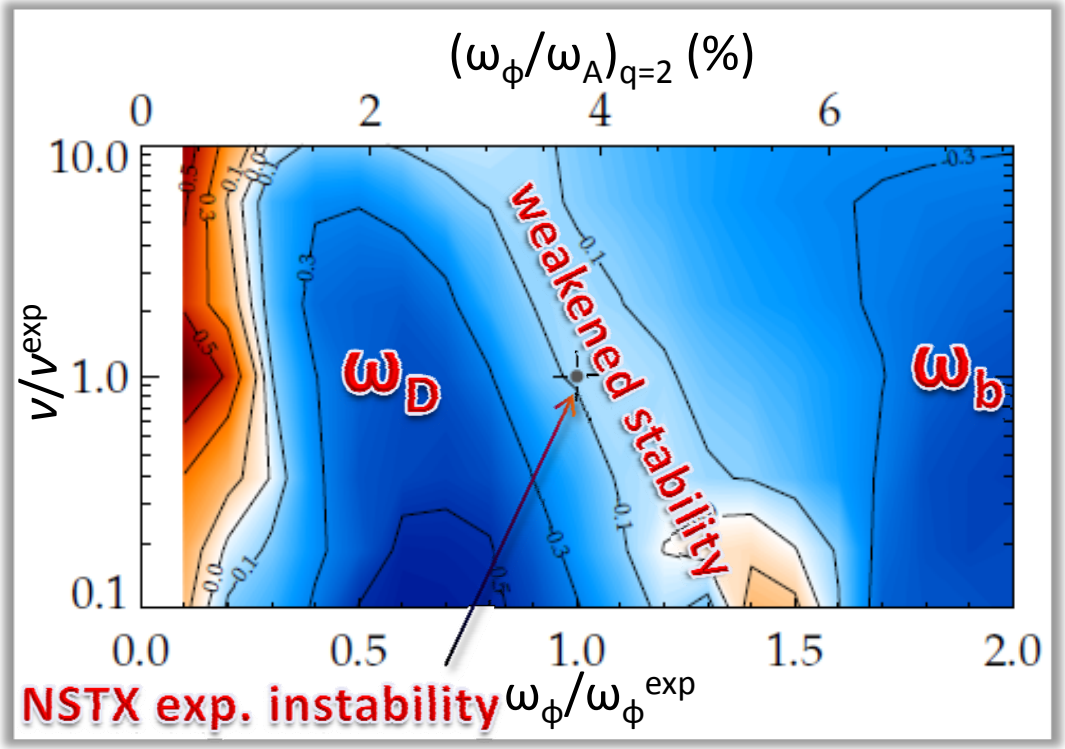

Visit the poster this afternoon for more detail

Abstract

Continuous, disruption-free operation of tokamaks requires stabilization of the resistive wall mode (RWM). Theoretically, the RWM is thought to be stabilized by energy dissipation mechanisms that depend on plasma rotation and other parameters, with kinetic effects being emphasized[1]. Experiments in NSTX show that the RWM can be destabilized in high rotation plasmas while low rotation plasmas can be stable, which calls into question the concept of a simple critical plasma rotation threshold for stability. The present work tests theoretical stabilization mechanisms against experimental discharges with various plasma rotation profiles created by applying non-resonant n=3 braking, and with various fast particle fractions. Kinetic modification of ideal stability is calculated with the MISK code, using experimental equilibrium reconstructions. Analysis of NSTX discharges with unstable RWMs predicts near-marginal mode growth rates. Trapped ions provide the dominant kinetic resonances, while fast particles contribute an important stabilizing effect. Increasing or decreasing rotation in the calculation drives the prediction farther from the marginal point, showing that unlike simpler critical rotation theories, kinetic theory allows a more complex relationship between plasma rotation and RWM stability. Results from JT-60U show that energetic particle modes can trigger RWMs[2]. Kinetic theory may explain how fast particle loss can trigger RWMs through the loss of an important stabilization mechanism. These results are applied to ITER advanced scenario equilibria to determine the impact on RWM stability.

[1] B. Hu et al., *Phys. Plasmas* **12** (2005) 057301. [2] G. Matsunaga et al., IAEA FEC 2008 Paper EX/5-2.

Non-linear inclusion of γ and ω_r in dispersion relation makes very little difference to MISK results

γ and ω_r appear non-linearly on both sides of the dispersion relation.

$$(\gamma - i\omega_r)\tau_w = -\frac{\delta W_\infty + \delta W_K}{\delta W_b + \delta W_K}$$

$$\delta W_K \sim \left[\frac{(\omega_r + i\gamma)\frac{\partial f}{\partial \varepsilon} + \frac{\partial f}{\partial \Psi}}{\langle \omega_D \rangle + l\omega_b - i\nu_{\text{eff}} + \omega_E - \omega_r - i\gamma}\right]$$

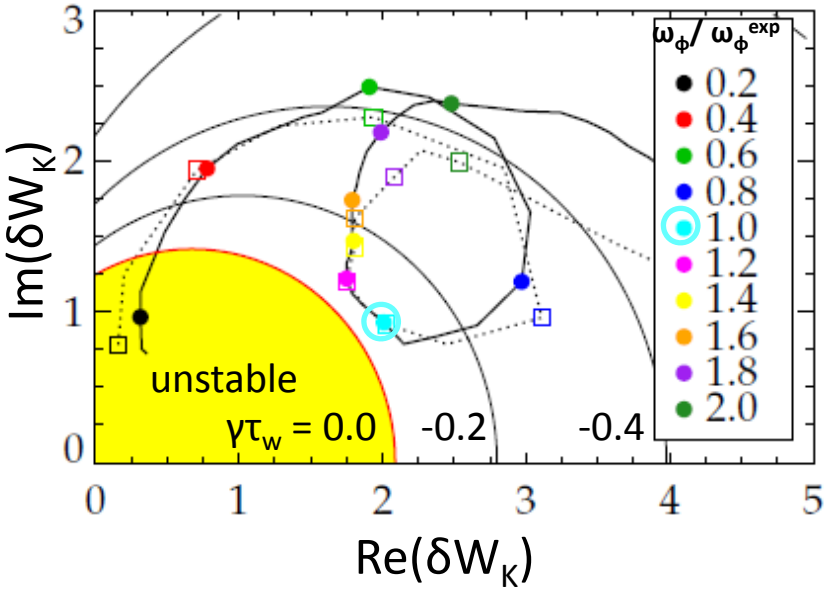

- MARS-K is self-consistent, MISK can use iteration to include the non-linear effect.
- Iteration with τ_w = 1ms (dashed line) makes very little difference to the result, especially when γ is small.

Improvements to the theory and calculation, to use as a quantitative predictor of instability

1. Examine sensitivity of calc.

- Non-linear inclusion of ω_r and γ: Iteration (τ_w = 1ms)
- Sensitivities to inputs: ex: $\Delta q = 0.15 - 0.25$

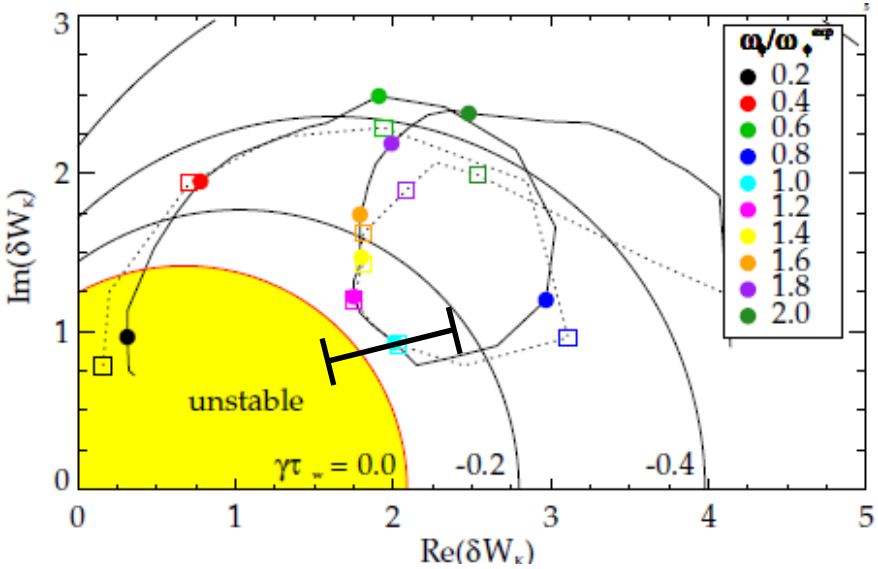

121083 @ 0.475 s

2. Include energetic particles

- Important stabilizing kinetic effects in theory
- E.P. modes known to "trigger" RWM in experiment

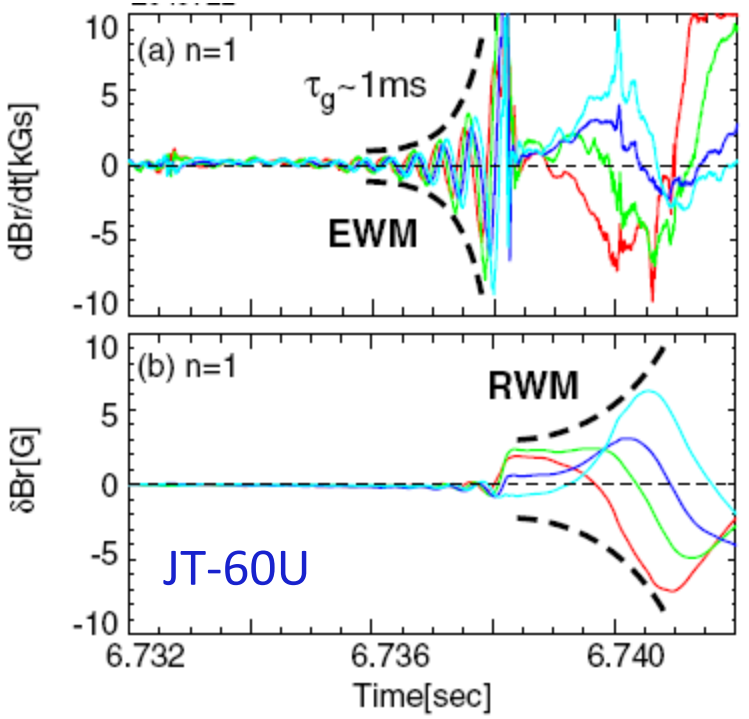

DIII-D experiment motivated by MISK results explored the effect of energetic particles on RWM stability

MISK Analysis

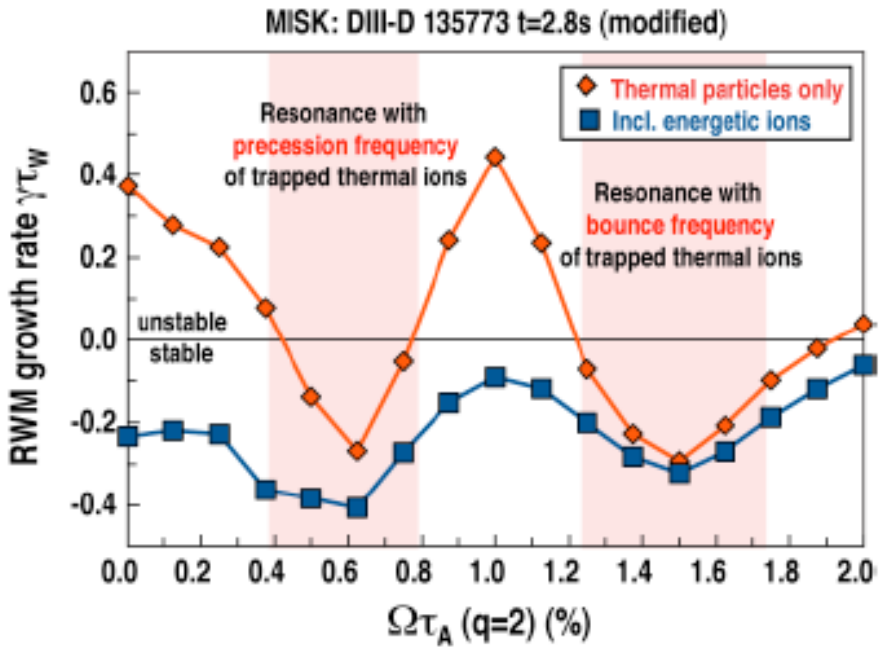

- Predicted instability inconsistent with experiment
- Adding energetic particles makes RWM stable - consistent
- Weakened ω_ϕ profile remains

DIII-D Experiment (with Reimerdes)

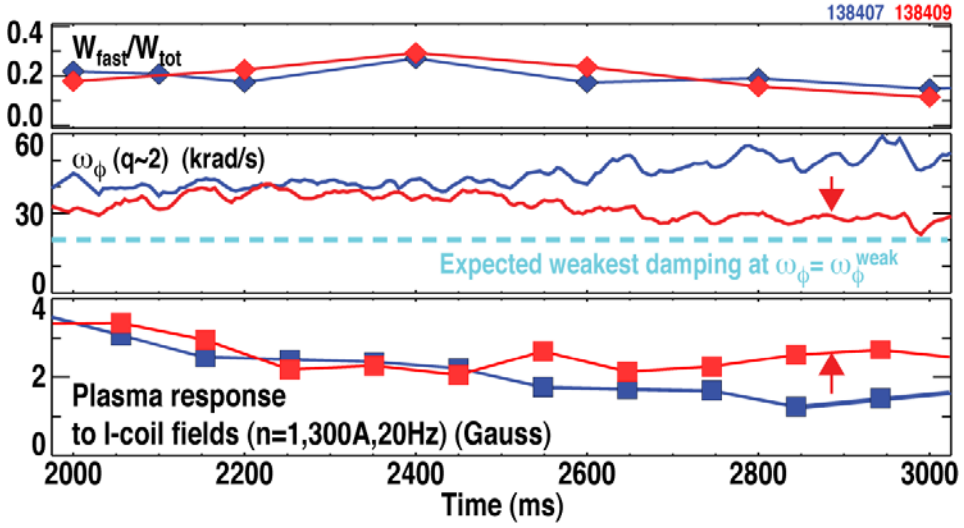

- Higher n_e and I_p reduced W_f/W_t by 40% over previous exp.
- RWM remains stable, but response higher as $\omega_\phi \rightarrow \omega_\phi^{weak}$

The RWM is identified in NSTX by a variety of observations

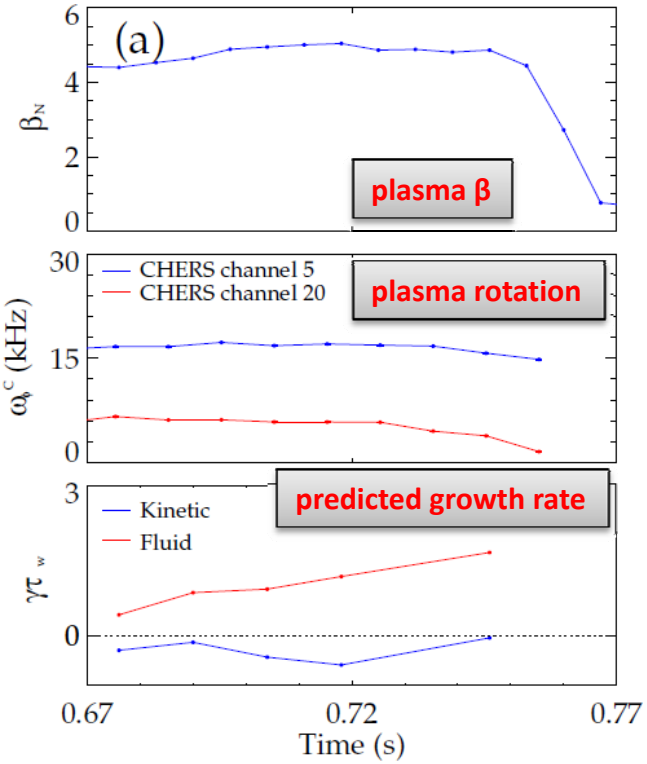

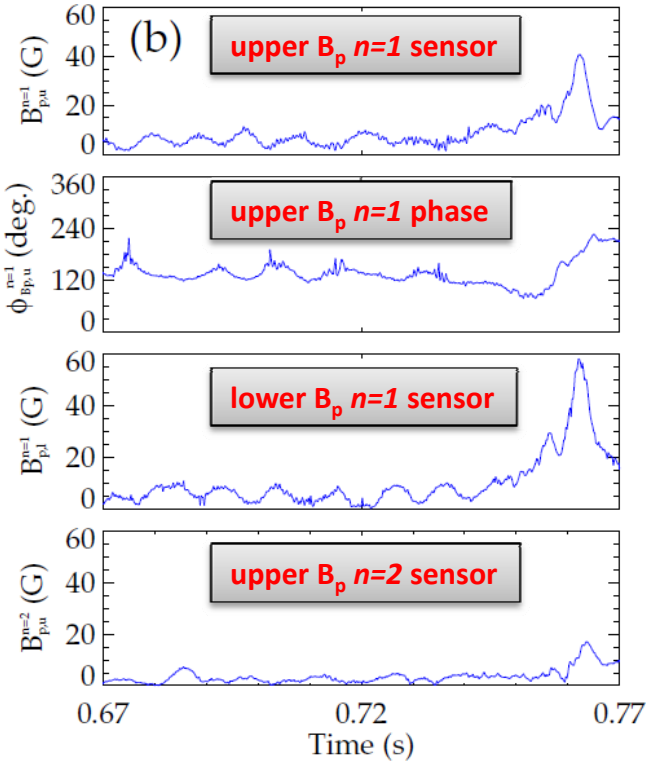

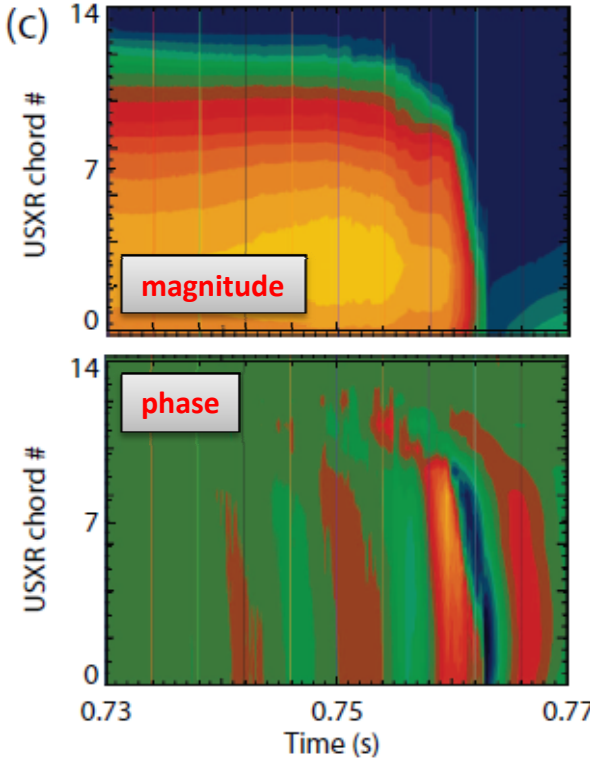

NSTX 130235 @ 0.746 s

- Change in plasma rotation frequency, ω_ϕ
- Growing signal on low frequency poloidal magnetic sensors
- Global collapse in USXR signals, with no clear phase inversion
- Causes a collapse in β and disruption of the plasma

NSTX 121083 @ 0.475 RWM characteristics

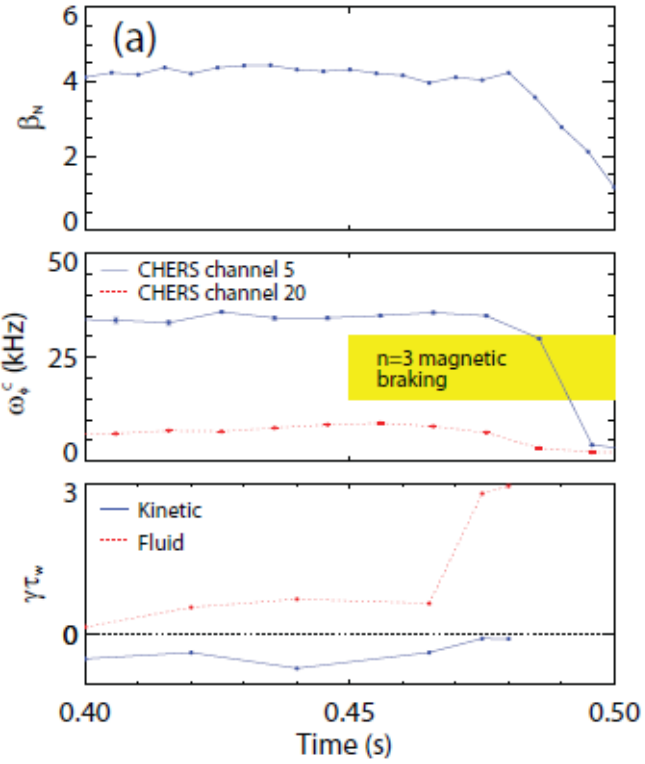

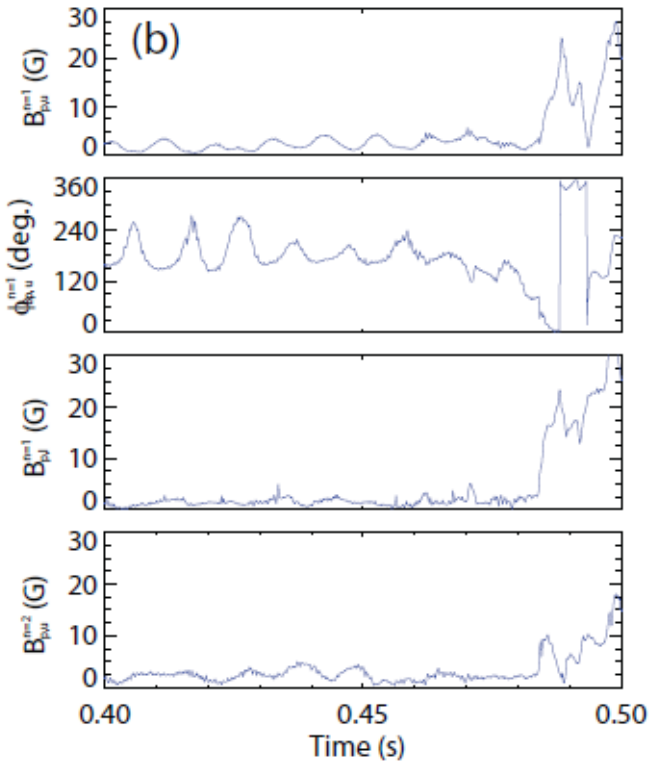

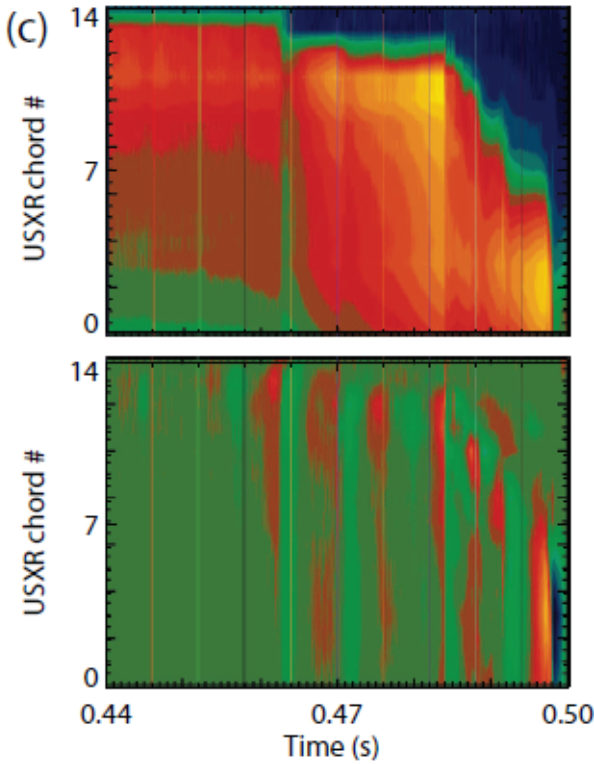

Present isotropic distribution function for energetic particles overestimates the trapped ion fraction

- First-order check:
  - MISK isotropic f overestimates the trapped ion fraction (compared to TRANSP).

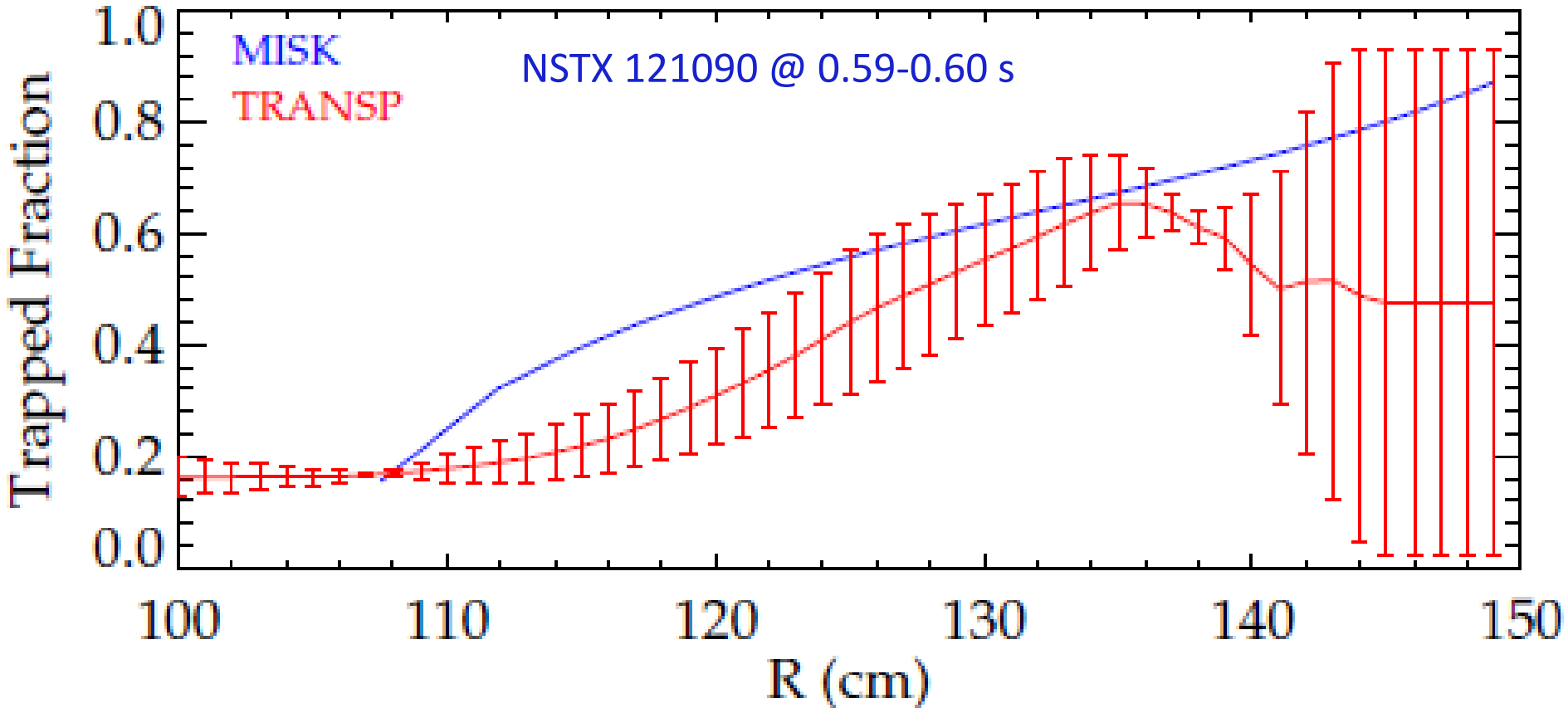

MISK sometimes overpredicts stability

unstable

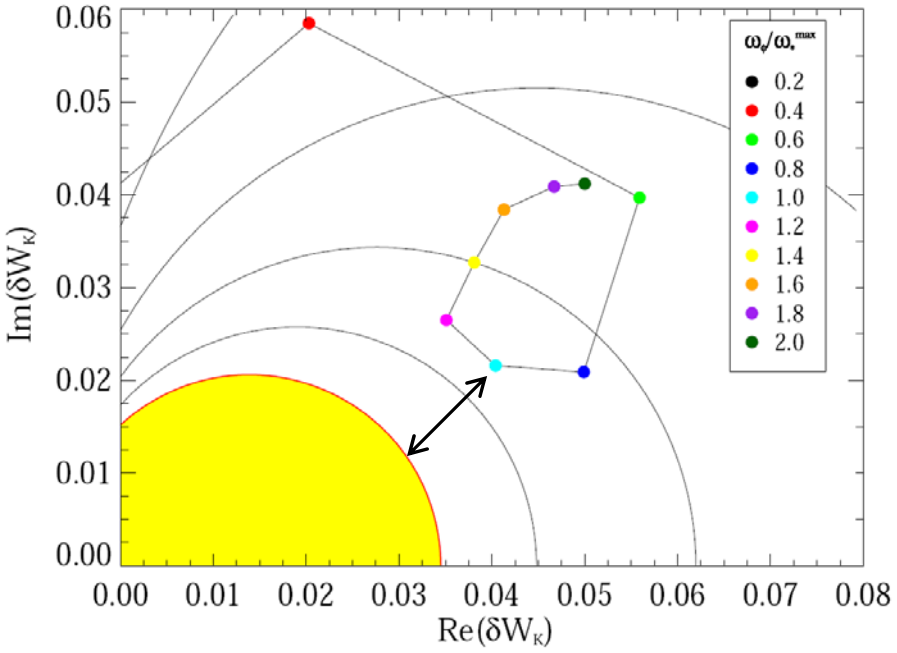

128856 @ 0.529

stable

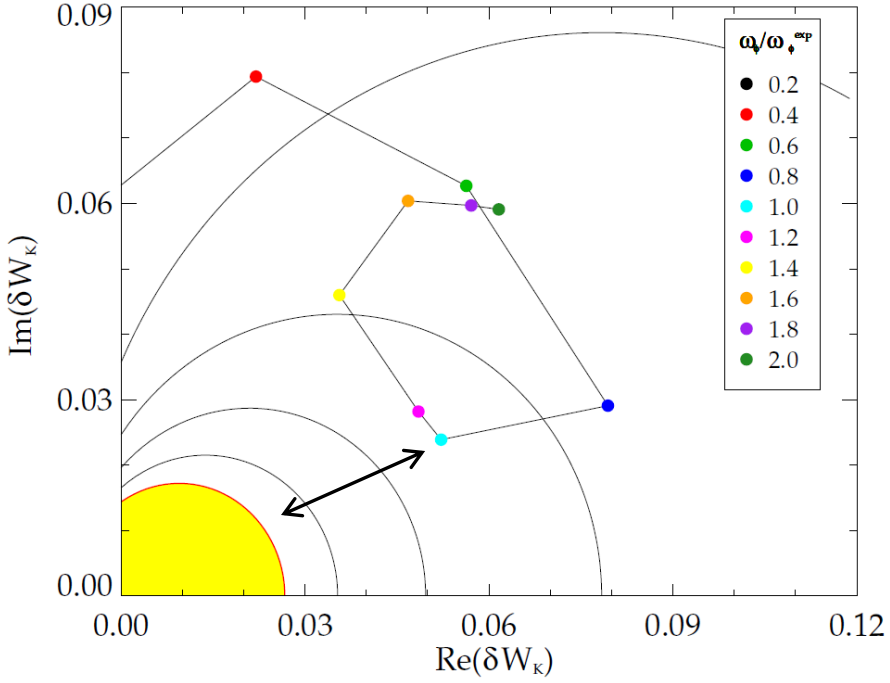

133367 @ 0.635

Perturbative vs. Self-consistent Approaches and Three Roots of the RWM Dispersion Relation

γ is found with a self-consistent or perturbative approach

The self-consistent (MARS) approach: solve for γ and ω from:

$$
\begin{aligned}
(\gamma + i(\omega_\phi - \omega))\tilde{\xi} &= \tilde{\mathbf{u}} - \mathbf{u_0}\cdot\nabla\tilde{\xi} \\
\rho(\gamma + i(\omega_\phi - \omega))\tilde{\mathbf{u}} &= \mathbf{j}\times\tilde{\mathbf{B}} + \tilde{\mathbf{j}}\times\mathbf{B} - \nabla\cdot\tilde{\mathbf{P}} - \rho\left(\mathbf{u_0}\cdot\nabla\tilde{\mathbf{u}} + \tilde{\mathbf{u}}\cdot\nabla\mathbf{u_0}\right) \\
\tilde{\mathbf{j}} &= \frac{1}{\mu_0}\boldsymbol{\nabla}\times\tilde{\mathbf{B}} \\
(\gamma + i(\omega_\phi - \omega))\tilde{\mathbf{B}} &= \nabla\times(\mathbf{u}\times\mathbf{B}) - \mathbf{u_0}\cdot\nabla\tilde{\mathbf{B}} \\
(\gamma + i(\omega_\phi - \omega))\tilde{\mathbf{P}} &= -\tilde{\mathbf{u}}\cdot\boldsymbol{\nabla}\mathbf{P} \\
\boldsymbol{\nabla}\cdot\tilde{\mathbf{P}} &= \boldsymbol{\nabla}\tilde{p} + \nabla\cdot\left[\tilde{p}_\perp^K\mathbf{I} + (\tilde{p}_\parallel^K - \tilde{p}_\perp^K)\hat{\mathbf{b}}\hat{\mathbf{b}}\right].
\end{aligned}
$$

The perturbative (MISK) approach: solve for γ and ω from:

$$(\gamma - i\omega)\tau_w = -\frac{\delta W_\infty + \delta W_K}{\delta W_b + \delta W_K}$$

with δW_∞ and δW_b from PEST. There are three main differences between the approaches:

1. The way that rational surfaces are treated.
2. Whether ξ is changed or unchanged by kinetic effects.
3. Whether γ and ω are non-linearly included in the calculation.

Rational surfaces are treated differently

The self-consistent (MARS) approach: solve for γ and ω from:

$$
\begin{aligned}
(\gamma + i(\omega_\phi - \omega))\tilde{\xi} &= \tilde{\mathbf{u}} - \mathbf{u_0} \cdot \nabla \tilde{\xi} \\
\rho(\gamma + i(\omega_\phi - \omega))\tilde{\mathbf{u}} &= \mathbf{j} \times \tilde{\mathbf{B}} + \tilde{\mathbf{j}} \times \mathbf{B} - \nabla \cdot \tilde{\mathbf{P}} - \rho\left(\mathbf{u_0} \cdot \nabla \tilde{\mathbf{u}} + \tilde{\mathbf{u}} \cdot \nabla \mathbf{u_0}\right) \\
\tilde{\mathbf{j}} &= \frac{1}{\mu_0} \boldsymbol{\nabla} \times \tilde{\mathbf{B}} \\
(\gamma + i(\omega_\phi - \omega))\tilde{\mathbf{B}} &= \nabla \times (\mathbf{u} \times \mathbf{B}) - \mathbf{u_0} \cdot \nabla \tilde{\mathbf{B}} \\
(\gamma + i(\omega_\phi - \omega))\tilde{\mathbf{P}} &= -\tilde{\mathbf{u}} \cdot \boldsymbol{\nabla} \mathbf{P} \\
\boldsymbol{\nabla} \cdot \tilde{\mathbf{P}} &= \boldsymbol{\nabla} \tilde{p} + \nabla \cdot \left[\tilde{p}_\perp^K \mathbf{I} + (\tilde{p}_\parallel^K - \tilde{p}_\perp^K) \hat{\mathbf{b}} \hat{\mathbf{b}}\right].
\end{aligned}
$$

MARS-K: "continuum damping included through MHD terms". This term includes parallel sound wave damping.

In MISK a layer of surfaces at a rational ±Δq is removed from the calculation and treated separately through shear Alfvén damping.

Unchanging ξ may be a good assumption

For DIII-D shot 125701, the eignfunction doesn't change due to kinetic effects.

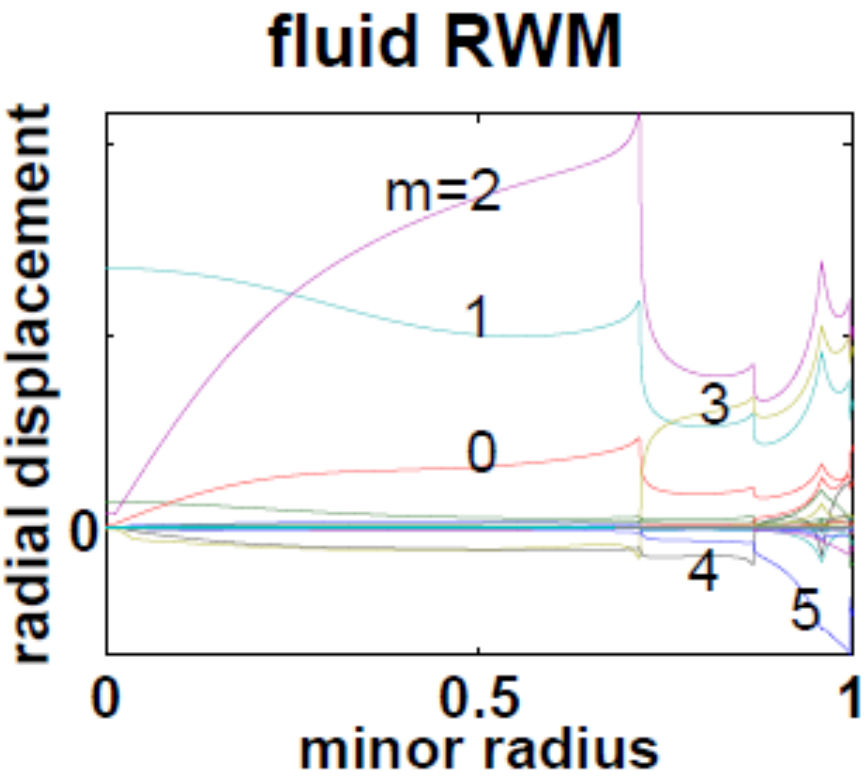

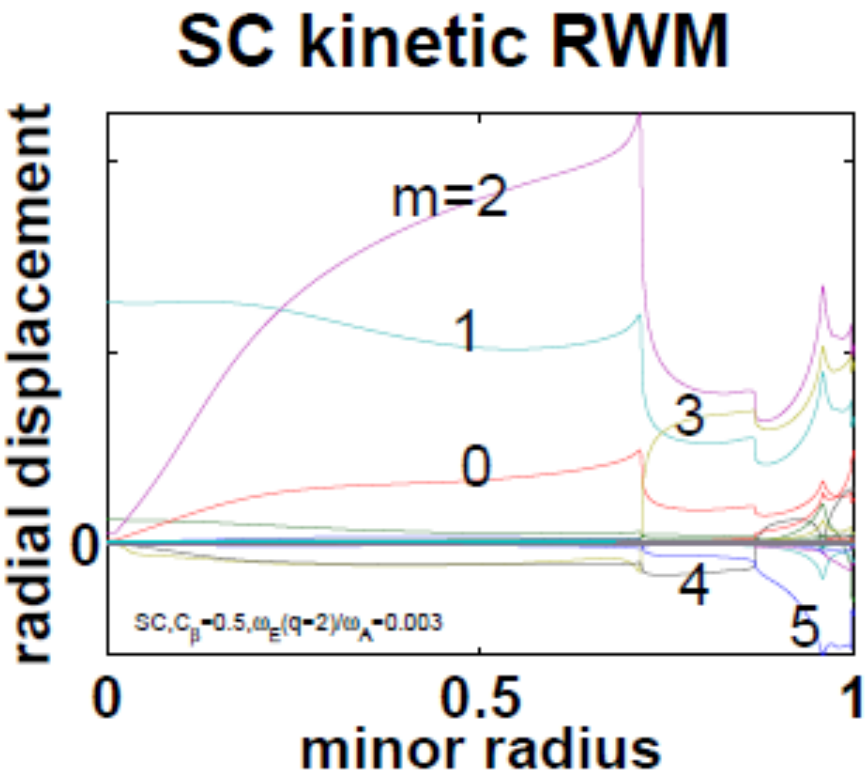

- *(Y. Liu, APS DPP 2008)*

Non-linear inclusion of γ and ω can be achieved in the perturbative approach through iteration

$$(\gamma - i\omega)\tau_w = -\frac{\delta W_\infty + \delta W_K}{\delta W_b + \delta W_K}$$

Example: NSTX 121083 @ 0.475

	τ_w = 0.1ms		τ_w = 0.5ms		τ_w = 1.0ms	
Iteration	γ	ω	γ	ω	γ	ω
0	-2577	-1576	-515	-315	-258	-158
1	-4906	431	-508	-172	-256	-139
2	-5619	800	-505	-177	-257	-140
3	-5745	828	-504	-179		
4	-5834	835				
5	-5855	838				
6	-5835	819				

The effect of iteration depends on the magnitudes of γ, ω

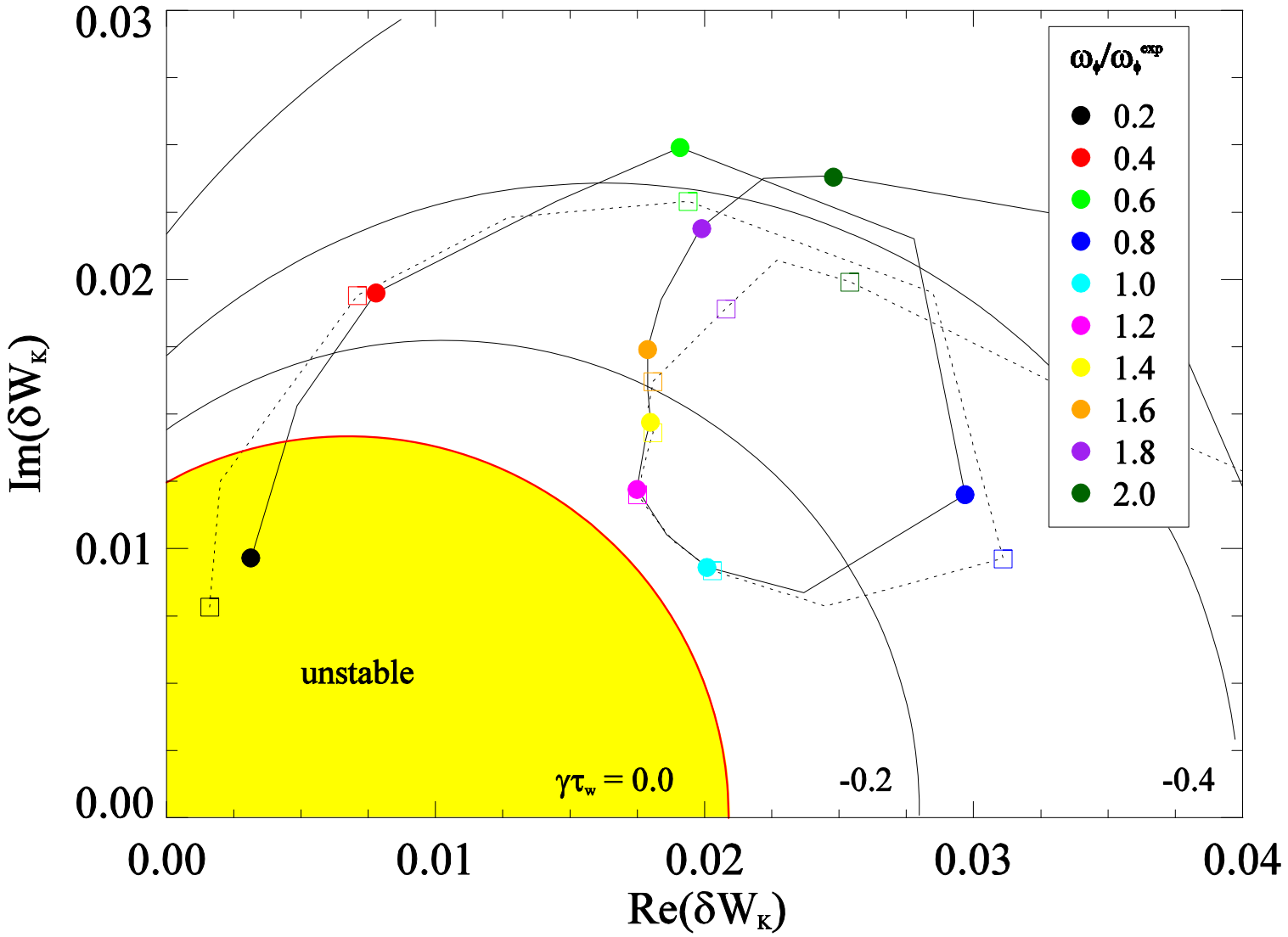

The dispersion relation has three roots

$$C = c_2 \int_0^\infty \left[\frac{\hat{\omega}_{*N} + (\hat{\varepsilon} - \frac{3}{2})\hat{\omega}_{*T} + \hat{\omega}_E + \hat{\omega} - i\hat{\gamma}}{\hat{\omega}_D \hat{\varepsilon}^a + \hat{\omega}_E + \hat{\omega} - i\hat{\gamma}} + \frac{-\hat{\omega}_{*N} - (\hat{\varepsilon} - \frac{3}{2})\hat{\omega}_{*T} + \hat{\omega}_E + \hat{\omega} - i\hat{\gamma}}{-\hat{\omega}_D \hat{\varepsilon}^a + \hat{\omega}_E + \hat{\omega} - i\hat{\gamma}} \right] \hat{\varepsilon}^{\frac{5}{2}} e^{-\hat{\varepsilon}} d\hat{\varepsilon}$$

Liu's simple example: a=0, c_2 = 0.18, ω_{*T} = 0

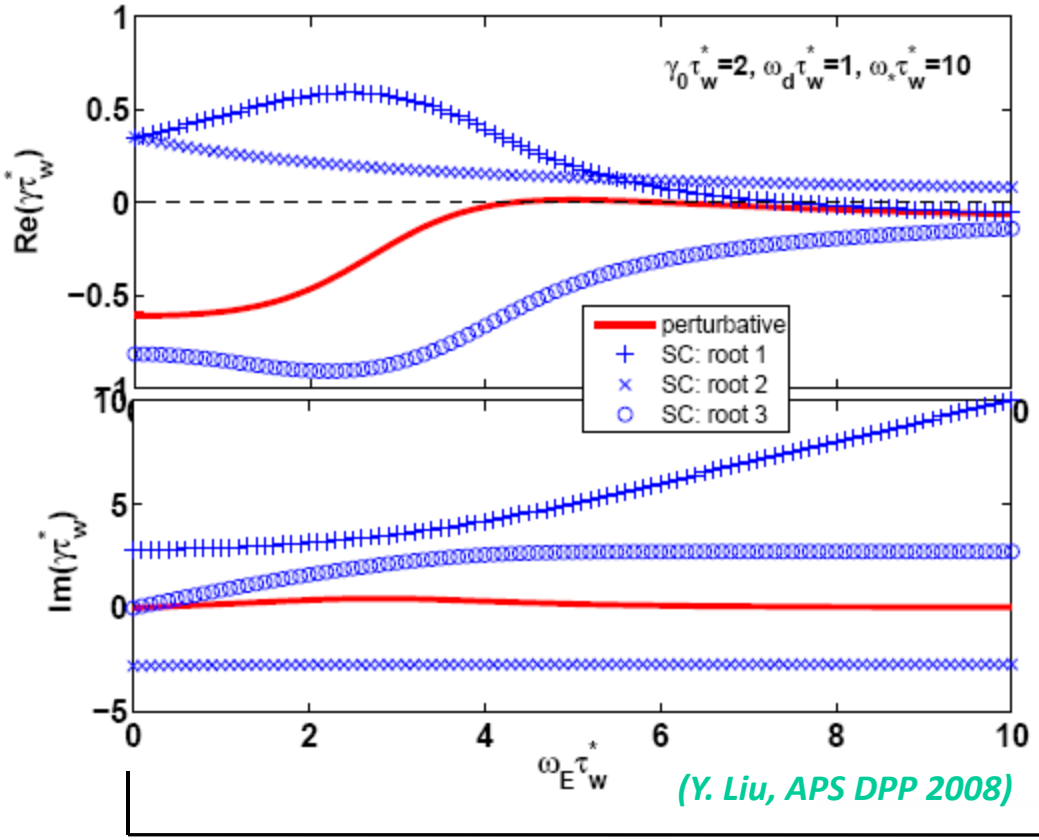

(Y. Liu, APS DPP 2008)

$$D = (\hat{\gamma} + i\hat{\omega})(\hat{\gamma}_f^{-1} + C) - 1 + C$$

Plot contours of 1/|D|

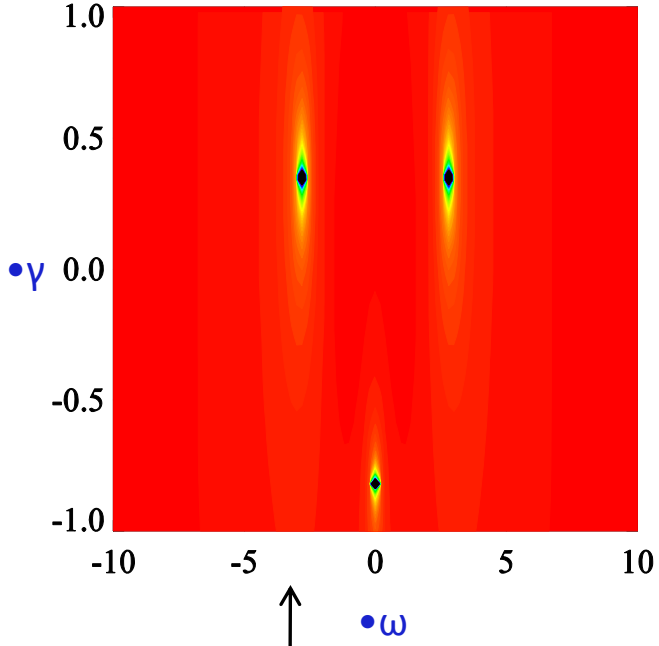

MISK and MARS-K Benchmarking

MISK and MARS-K were benchmarked using a Solov'ev equilibrium

$$\mu_0 P(\psi) = -\frac{1+\kappa^2}{\kappa R_0^3 q_0}\psi, \quad F(\psi) = 1$$

$$\psi = \frac{\kappa}{2R_0^3 q_0}\left[\frac{R^2 Z^2}{\kappa^2} + \frac{1}{4}\left(R^2 - R_0^2\right)^2 - a^2 R_0^2\right]$$

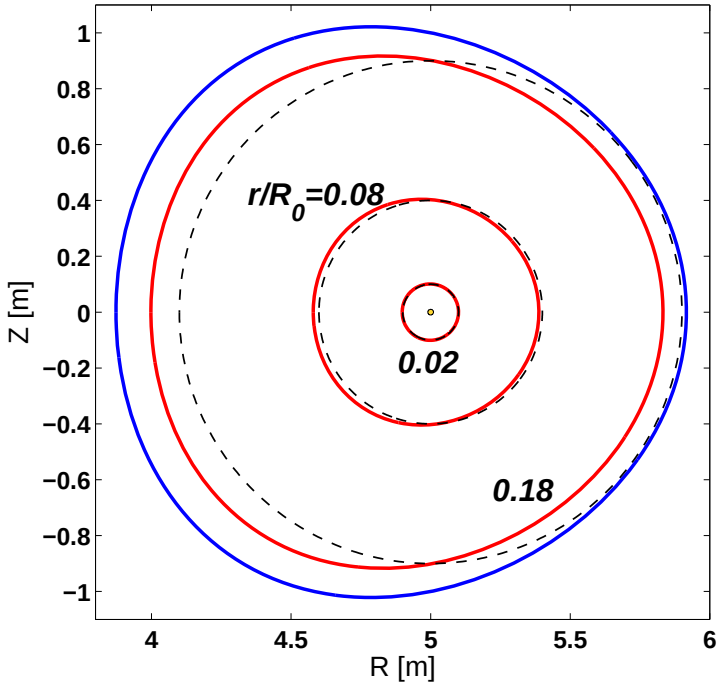

(Liu, ITPA MHD TG Meeting, Feb. 25-29, 2008)

- Simple, analytical solution to the Grad-Shafranov equation.
- Flat density profile means $\omega_{*N} = 0$.
- Also, ω, γ, and ν_{eff} are taken to be zero for this comparison, so the frequency resonance term is simply:

$$\delta W_K \propto \int \left[\frac{\left(\hat{\varepsilon} - \frac{3}{2}\right)\omega_{*T} + \omega_E}{\langle\omega_D\rangle + l\omega_b + \omega_E}\right] \hat{\varepsilon}^{\frac{5}{2}} e^{-\hat{\varepsilon}} d\hat{\varepsilon}$$

MARS-K: ***(Liu, Phys. Plasmas, 2008)***

Drift frequency calculations match for MISK and MARS-K

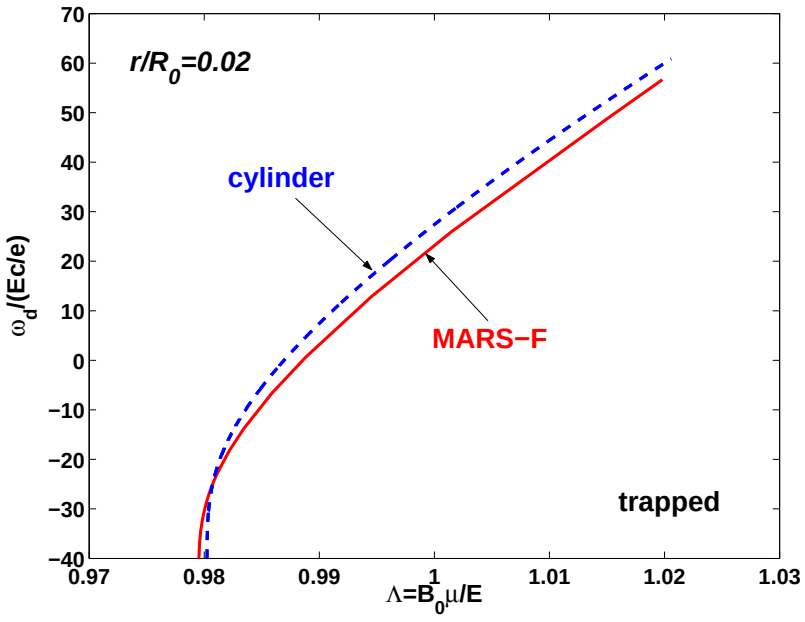

MARS

(Liu, ITPA MHD TG Meeting, Feb. 25-29, 2008)

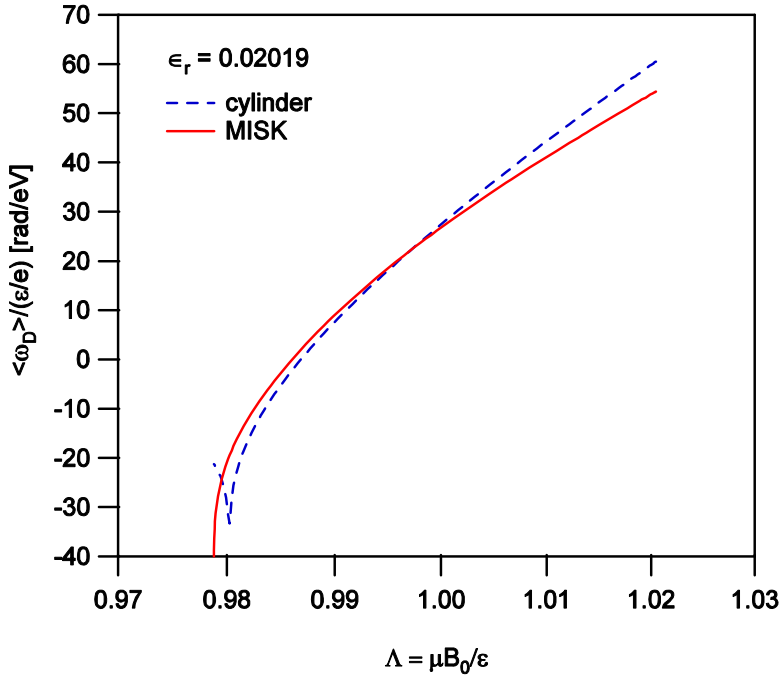

MISK

large aspect ratio approximation *(Jucker et al., PPCF, 2008)*

$$\frac{\langle \omega_D \rangle}{\varepsilon/e} = \frac{2q\Lambda}{R_0^2 B_0 \epsilon_r}\left[(2s+1)\frac{E\left(k^2\right)}{K\left(k^2\right)} + 2s\left(k^2-1\right) - \frac{1}{2}\right] \qquad k = \left[\frac{1-\Lambda+\epsilon_r\Lambda}{2\epsilon_r\Lambda}\right]^{\frac{1}{2}}$$

here, ϵ_r is the inverse aspect ratio, s is the magnetic shear, K and E are the complete elliptic integrals of the first and second kind, and $\Lambda = \mu B_0/\varepsilon$, where μ is the magnetic moment and ε is the kinetic energy.

Bounce frequency calculations match for MISK and MARS-K

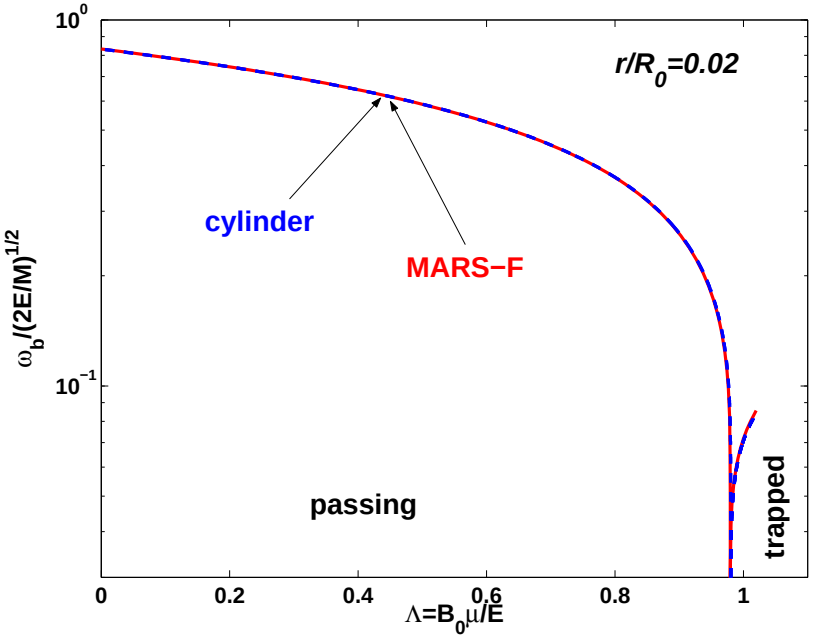

MARS

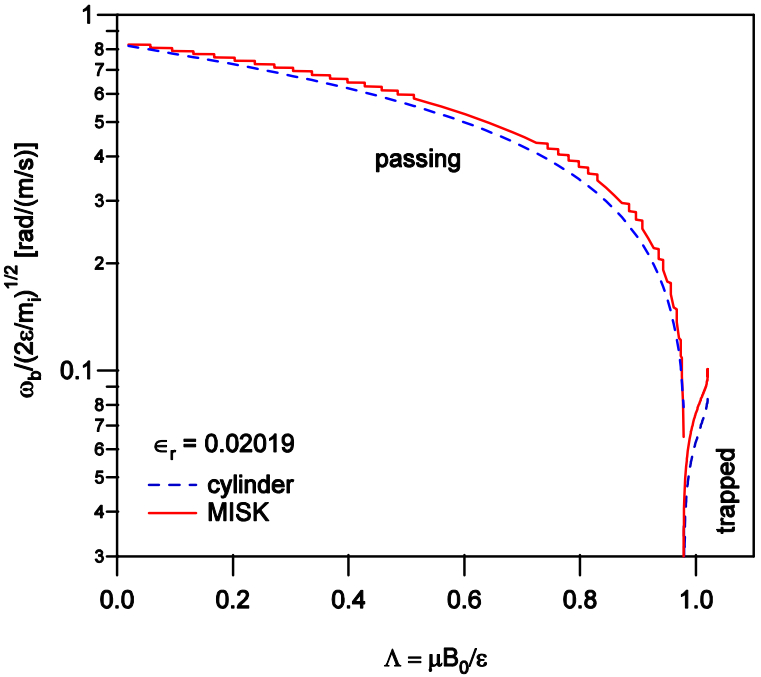

MISK

(Liu, ITPA MHD TG Meeting, Feb. 25-29, 2008)

large aspect ratio approximation *(Bondeson and Chu, PoP, 1996)*

$$\frac{\omega_b}{\sqrt{2\varepsilon/m_i}} = \frac{\sqrt{2\epsilon_r\Lambda}}{4qR_0}\frac{\pi}{K(k)} \quad \text{(trapped)} \qquad \frac{\omega_b}{\sqrt{2\varepsilon/m_i}} = \frac{\sqrt{1-\Lambda+\epsilon_r\Lambda}}{2qR_0}\frac{\pi}{K(1/k)} \quad \text{(circulating)}$$

$$k = \left[\frac{1-\Lambda+\epsilon_r\Lambda}{2\epsilon_r\Lambda}\right]^{\frac{1}{2}}$$

MISK and MARS-K match well at reasonable rotation

Good match for trapped ions and electrons at high rotation, but poor at low rotation.

The simple frequency resonance term denominator causes numerical integration problems with MISK that don't happen with realistic equilibria.

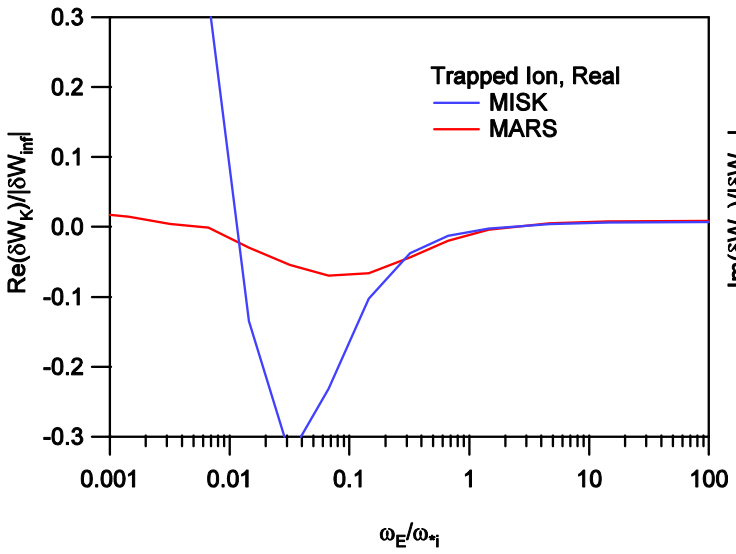

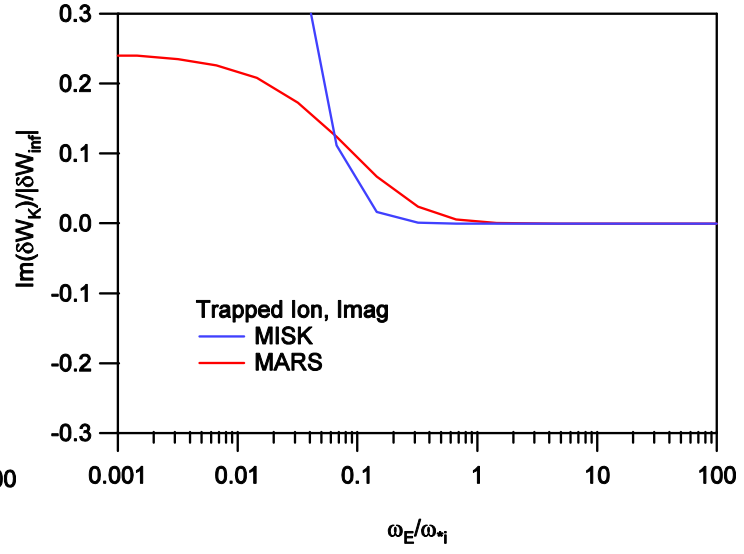

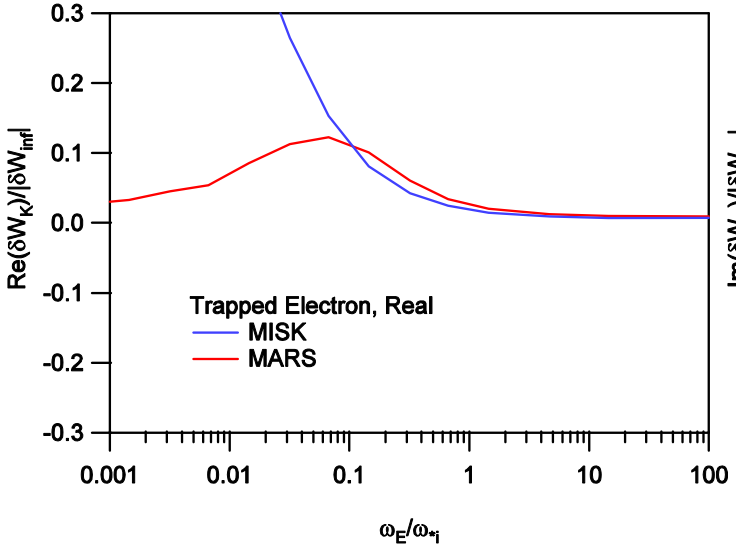

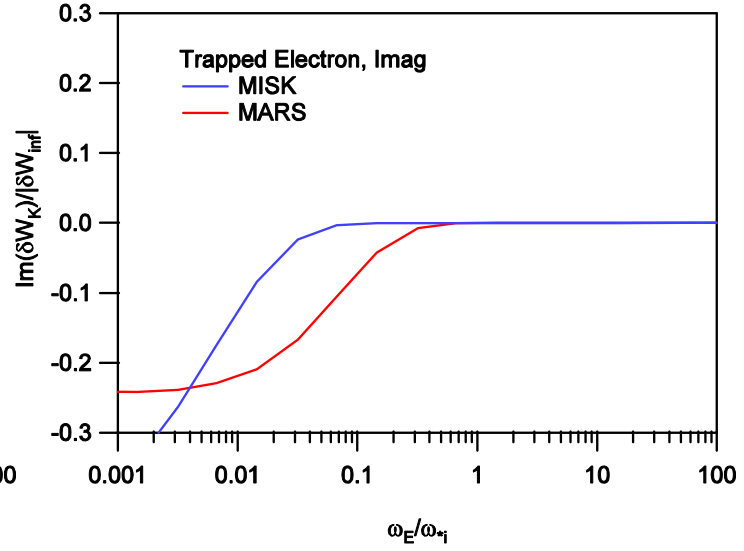

DIII-D Energetic Particle Experiment

MISK calculations indicate importance of energetic ions for RWM stability in low rotation DIII-D plasmas

[D3D MP 2009-99-07 by Reimerdes, Berkery, et al.]

- **Kinetic calculations using thermal particles only predict RWM to be most unstable at finite rotation**
  - Resonance with **precession frequency** of trapped particles at lower rotation
  - Resonance with **bounce frequency** of trapped particles at higher rotation
  - → RWM least stable for profile with $\Omega\tau_A \sim 1\%$ at $q=2$

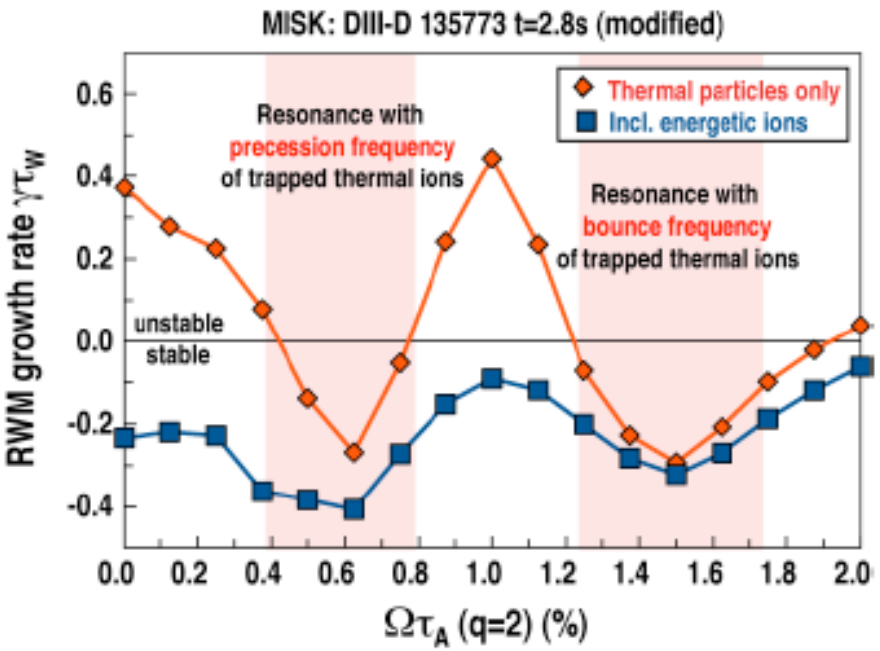

- **Trapped energetic ions (W_{fast}/W_{tot} ~23%) predicted to stabilize the equilibrium across the entire (low) rotation range**
  - Rotation dependence smeared out by resonance with precession frequency with trapped energetic ions
  - Low rotation wall stabilized plasmas typically have W_{fast}/W_{tot}>30%

Recent experiment tests kinetic stability models by reducing the energetic ion content

[D3D MP 2009-99-07 by Reimerdes, Berkery, et al.]

- An exploratory experiment succeeded in lowering W_{fast}/W_{tot} from ~35% to ~20%
  - Higher density
  - Higher plasma current
- RWM remains stable but an increased plasma response to applied *n*=1 field indicates weaker stabilization at lower plasma rotation Ω

→ Further experiments should look for a maximum in the amplification at finite rotation

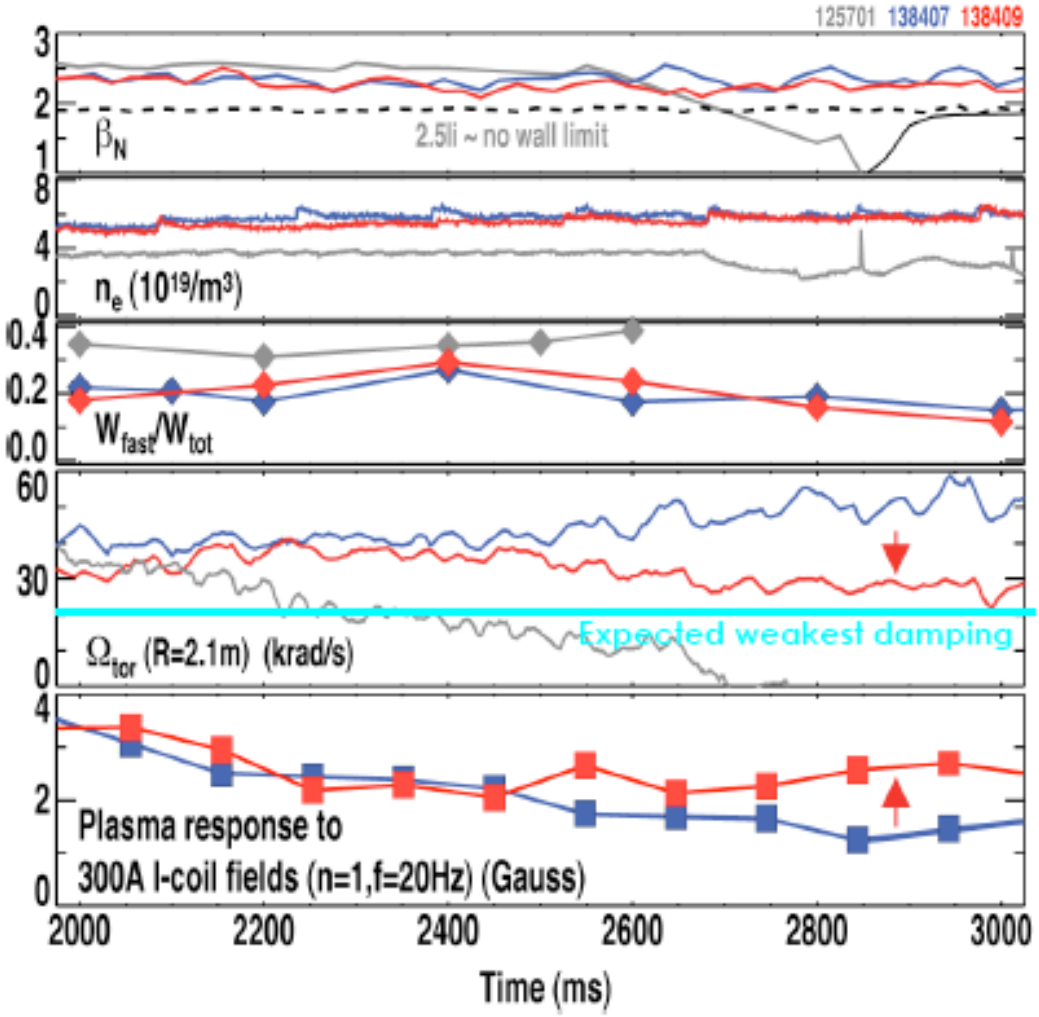

δW_K in the limit of high particle energy

Writing δW_K without specifying f:

$$\delta W_K = -\sqrt{2}\pi^2 \sum_{\pm\sigma} \sum_{l=-\infty}^{\infty} \int d\varepsilon \int d\Lambda \int d\Psi m^{-\frac{3}{2}} \frac{\hat{\tau}}{B_0} \frac{(\omega_r + i\gamma)\frac{\partial f}{\partial \varepsilon} + \frac{\partial f}{\partial \Psi}}{\langle \omega_D \rangle + l\omega_b - i\nu_{\text{eff}} + \omega_E - \omega_r - i\gamma} \varepsilon^{\frac{5}{2}} |\langle HT/\varepsilon \rangle|^2$$

Rewriting with explicit energy dependence:

$$\delta W_K = -\sqrt{2}\pi^2 \sum_{\pm\sigma} \sum_{l=-\infty}^{\infty} \int d\varepsilon \int d\Lambda \int d\Psi m^{-\frac{3}{2}} \frac{\hat{\tau}}{B_0} \frac{(\omega_r + i\gamma)\frac{\partial f}{\partial \varepsilon} + \frac{\partial f}{\partial \Psi}}{\varepsilon\langle \omega_D \rangle + l\sqrt{\varepsilon}\omega_b - i\varepsilon^{-\frac{3}{2}}\nu_{\text{eff}} + \omega_E - \omega_r - i\gamma} \varepsilon^{\frac{5}{2}} |\langle HT/\varepsilon \rangle|^2$$

So that, for energetic particles, where ε is very large:

$$\delta W_K = -\sqrt{2}\pi^2 \sum_{\pm\sigma} \sum_{l=-\infty}^{\infty} \int d\varepsilon \int d\Lambda \int d\Psi m^{-\frac{3}{2}} \frac{\hat{\tau}}{B_0} \frac{(\omega_r + i\gamma)\frac{\partial f}{\partial \varepsilon} + \frac{\partial f}{\partial \Psi}}{\varepsilon\langle \omega_D \rangle + l\sqrt{\varepsilon}\omega_b - i\varepsilon^{-\frac{3}{2}}\nu_{\text{eff}} + \omega_E - \omega_r - i\gamma} \varepsilon^{\frac{5}{2}} |\langle HT/\varepsilon \rangle|^2$$

large

large

large

Note: this term is independent of ε.

XXX